SINTEF Energi AS
Postadresse:
Postboks 4761 Torgarden
7465 Trondheim

Sentralbord: 45456000

energy.research@sintef.no

Foretaksregister:
NO 939 350 675 MVA

Memo

DExpand Case Studies: WP1 System modeling and optimization

SAKSBEHANDLER / FORFATTER
Rubén Mocholí Montañés
Donghoi Kim
Luca Riboldi

	BEHANDLING	UTTALELSE	ORIENTERING	ETTER AVTALE
GÅR TIL				
DExpand Consortium				

PROSJEKTNR / SAK NR	DATO	GRADERING
DExpand	2021-09-06	Fortrolig

Abstract

Whilst the focus of the DExpand project is developing efficient and cost-effective expander designs, it is of importance to define what are the boundary conditions in which those expanders will have to perform. System modelling, simulation and optimization becomes fundamental to define those conditions. Process design and optimization of heat-to-power cycles is a developed research area. Several studies dealt with the conversion of various sources of waste heat into power by means of different cycles and working fluids.

The DExpand WP1 deals with system modeling and optimization and case studies for small scale ORC systems. Several technical meetings were held with the consortium early in in 2021 in order to jointly define the cases, define the modeling tools and constraints for modeling and optimization. This short Memo presents the main results from optimization work and methodology chosen for Phase 1 in WP1.

The optimization results and expander design analysis indicate the dimension and rotating speed of the turbomachinery is within the typical design range of such small gas expanders. Thus, the results from Phase 1 part of WP1 give input parameters to WP2 that could be used as first estimate boundary and operating conditions for detail expander design in other work packages. As the expander design activities in WP2 proceed, further communication between WP1 and WP2 are envisaged to refine and mutually strengthen the work.

1 Introduction

The DExpand project WP1 includes a methodology to translate process performances into expander design parameters through system modelling, simulation and optimization. The main objective of the first phase in WP1 is to design three different heat-to-power conversion cycles by means of system modelling, simulation and optimization. The work included the following:

- Definition of case studies
- Definition of performance targets and KPIs
- Modelling and optimization of processes
- Results: Inputs available for expander design (WP2)

2 Definition of Case Studies

The main objective within WP1 is to design three different organic Rankine cycles (ORCs) by means of system modelling, simulation and optimization. The work includes defining case studies and in detail specific boundary conditions and their operating range, for three different applications with expander power output in the range of 1–50 kW.

The three case studies are be based on:

1) biogas-driven engine waste heat recovery
2) low-temperature geothermal heat source
3) biomass-fired micro-cogeneration

2.1 Case Study 1: ORC for biogas internal combustion engine flue gas for distributed Energy Systems

Several case studies were proposed early in the project for further evaluation in DExpand as industrial waste heat case, including:

- Industrial waste heat (aluminum production) case study.
- Ship engine jacket water case study.
- Biogas WHR case study.

Aluminum case is based on the flue gas available. However, it is considered challenging to exploit the waste heat source in an efficient manner due to low energy density and relatively high fan power requirements. Other heat sources with higher temperature levels are more challenging to be exploited (e.g., heat from walls). The ship case as was presented might result in a power output (> 200 kW) slightly higher than the main project scope (scale of expanders to be developed for efficient and cost-effective expander designs in DExpand). Applications for smaller ships might be in the original range (< 100 kW). However, the biogas WHR case study was selected after several discussions within the DExpand consortium.

There are efforts being held in several EU countries to develop micro scale biogas plants using only on farm biomass resources for energy production as a new and potentially more sustainable renewable energy technology. An example is biogas from anaerobic digestion in farms. Internal combustion engines ICEs can make use of generated biogas as fuel for heat and power production in ICEs. This makes sense in the context of distributed energy systems (DES), where the biogas is used onsite. Small scale ORC can be installed to recover waste heat from flue gas of ICE and possible cooling water (jacket cooling water) to produce extra heat and power as shown in Figure 1.

Typically, 20-50% of the produced heat from the WHR system of the ICE will be required for heating, both the fermentor and other buildings and processes. The heat demand will be however seasonally dependent, suggesting different utilization methods of the waste heat sources (flue gas and jacket water). In this work, the heat demand is assumed to be covered by the jacket water while the flue gas is used to produce electricity through an ORC system. More details on specific plant conditions can be found in Chapter 3.2.

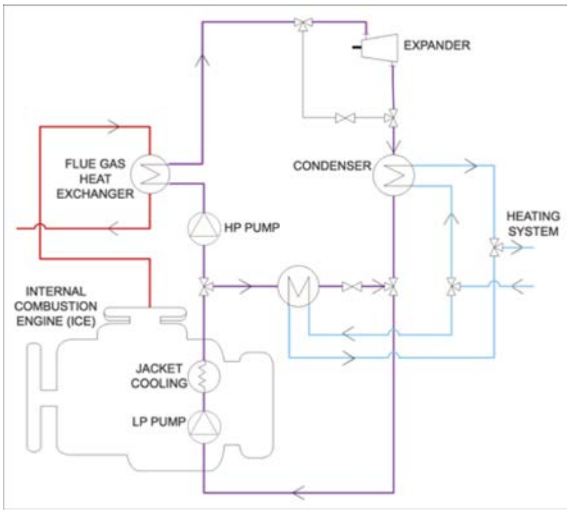

Figure 1. Possible configuration of the ORC system for Biogas driven ICE.

2.2 Case Study 2: ORC for Low temperature geothermal heat source from deep energy wells

The increasing concern on environment problems has led to the development of renewable energy sources, being the geothermal energy one of the most promising ones in terms of power generation. Due to the low heat source temperatures this energy provides, the use of Organic Rankine Cycles is a possibility to guarantee a good performance of the system. In the paper by Encabo et al.[1], the optimization of such ORC system was carried out to determine the most suitable working fluid. In DExpand, NTNU provided the case study parameters and boundary conditions for the system modelling, design and optimization work. In addition, technical constraints for the experimental rig "Expand" were provided. The working Fluid: R600a (iso-butane) has been pre-selected in previous work, as it will be the one tested in the Expand rig. The work should make sure that the resulting expander gross power output is below 50kW to fit the scope of the project on small scale expanders. More details on plant conditions are suggested by NTNU as shown in Chapter 3.2.

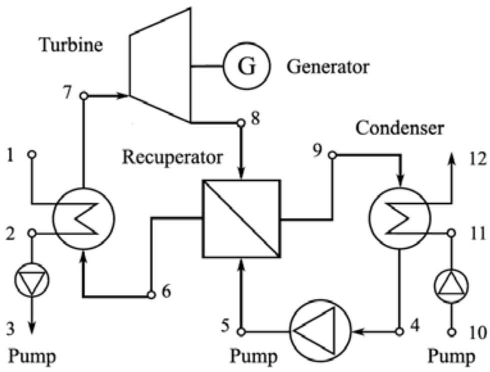

Figure 2. Schematic diagram of the ORC for Case Study 2.

[1] Encabo-Cáceres, Agromayor, Nord, Thermodynamic Optimization of an Organic Rankine Cycle for Power Generation from a Low Temperature Geothermal Heat Source. Proceedings of the 58th SIMS September 25th - 27th 2017, Reykjavik, Iceland.

2.3 Case Study 3: ORC for biomass fired micro-cogeneration of heat and power

Regarding the biomass micro-CHP system, the number of systems utilizing solid and lower quality fuels is very low, even though the supply of those fuels can be significant, reliable and their price may be low. Only a few units and projects for µCHP systems operating with solid fuels (biomass) and having power output < 30 kW_e have been conducted in the world. Systems integrating biomass utilization with the power production in a single unit, without need to obtain and combine various technologies, were very few and are mostly discontinued. Currently there are new companies with micro-ORC modules, where the biomass boiler and accessories have to be eventually handled separately by the customer.

CTU provides case study parameters and boundary conditions in Chapter 3.2. In addition, technical constraints for cycle design based on the experimental rig are provided based on the µCHP ORC rig. Indeed, CTU has two biomass (woodchip) fired ORC systems. The working fluid is MM (hexametyl disiloxane). More details on plant conditions are shown in Chapter 3.2.

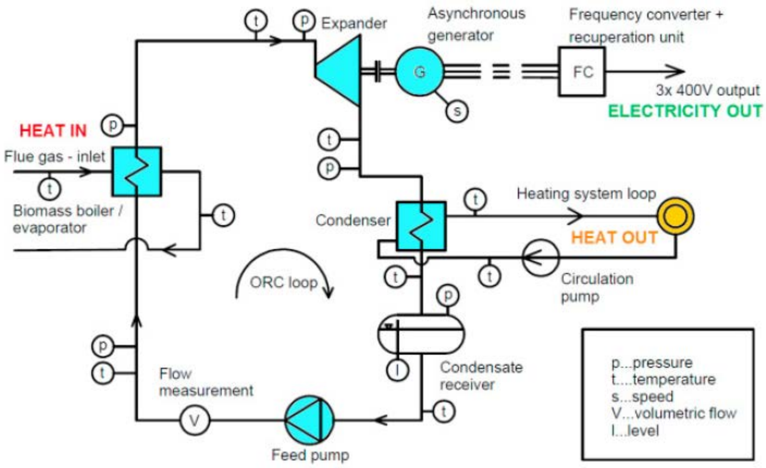

Figure 3 Schematic diagram of the ORC for Case Study 3.

3 Method

Three case studies are defined for small scale heat-to-power ORC system design and optimization. The cases will define the boundary conditions for optimization, together with possible cycle configurations, inequality constraints and independent variables for the optimization.

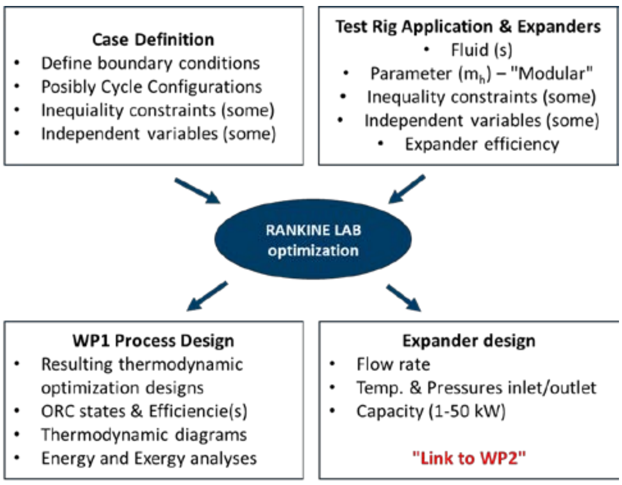

Figure 4. Method basis for DExpand WP1 Phase 1.

3.1 Process synthesis

Table 1 summarizes the case studies, the definition of the processes to be optimized, considering the following aspects:

- <u>Process configuration:</u> Simple process configurations will be preferred for these small-scale distributed applications (due to techno-economic and scale limitations and constraints). Accordingly, the results are provided for simple cycle and for cycle with recuperator.
- <u>Working fluids:</u> The working fluids for Case 2 and 3 are predefined by the design and rig constraints, since the rigs are tailor made to those specific working fluids. Case 1 will also use the same working fluid as Case 3 since they have similar operating conditions.
- <u>Rigs:</u> The rigs from NTNU and CTU define some boundary conditions.
- <u>Expanders:</u> The expanders are relevant as they will define a preliminary efficiency value to be set in optimizations.
- <u>Thermodynamic boundary conditions</u>: depend on the case study.

Table 1. Summary of main aspects related to process synthesis for the three case studies in DExpand.

Case	Case 1: Biogas ICE WHR	Case 2: Low temperature geothermal	Case 3: Biomass micro-CHP
Process Configuration	Simple cycle with or without recuperator	Simple cycle with or without recuperator	Simple cycle with or without recuperator
Working fluid	MM	Isobutane	MM
Test Rig	assumed as CTU	Expand	CTU
Objective KPI	Net power output	Net power output	Net power output
Design basis	Design 1. Test rig constraints Design 2. Practical constraints	Design 1. Test rig constraints Design 2. Practical constraints	Design 1. Test rig constraints Design 2. Practical constraints
Expander type/efficiency	Design expander: Relevant to test rig (CTU)	Design expander: Relevant to test rig	Design expander: Relevant to test rig

3.2 DExpand design basis

The optimization was performed for the case studies according to two different design bases.

Design 1 – rig constraints:
The first design basis allows to identify the thermodynamic optimum with rig constraints. The rig constraints include cycle variables that must be constrained to suit the test rigs specific characteristics. Therefore, Design 1 will consider a more limited range of operating conditions, including the need for subcritical working fluid operating conditions. The optimum solution obtained with Design 1 will directly provide indications on the conditions at which the expanders will be designed, optimised and tested in WP2.

Design 2 – practical constraints:
The second design basis represents the thermodynamic optimum with practical constraints. The practical constraints include limitations to the cycle parameters and operating conditions that are given by the utilization of state-of-the-art equipment. Given the inherent limitations of lab facilities, these constraints are expected to be less stringent than the rig constraints in Design 1. The objective of Design 2 optimization

is indeed to evaluate the potential of the ORC systems in actual operating conditions and to provide a second set of boundary conditions for the design of the expanders.

3.2.1 Case Study 1: Biogas ICE WHR ORC

To define the heat sources, BGA 136 Engine[2] is selected to represent a biogas driven internal combustion engine. This engine delivers 140 kWth through the heat exchanger for flue gas WHR, which is suitable for expander capacity below 50 kW. Based on the engine datasheet shown in Table 2, the flue gas composition is calculated by assuming a biogas composition of 50 mol% CH_4 and 50 mol% CO_2.

Table 2. BGA 136 Engine datasheet for Biogas ICE WHR ORC systems and estimated flue gas composition.

Item	Unit	Value
Fuel	-	50 mol% CH_4
Fuel flow rate	Nm^3/ h	101.0
Exhaust Gas Flow	kg/h	1043
Exhaust gas temperature	°C	580
Exhaust gas WHR outlet temperature	°C	160
Thermal output of 160 °C exhaust gas	kWth	140
Estimated flue gas composition		
CO_2	mol%	12.583
H_2O	mol%	12.583
N_2	mol%	69.052
O_2	mol%	5.782

Case Study 1 focuses on producing electricity from flue gas, considering a warm climate condition or summer season. Thus, instead of heating water, cooling water is used as a heat sink. Hexametyldisiloxane (MM) is selected as the working fluid for the ORC since this case has similar heat source conditions as Case Study 3. To avoid the degradation of the working fluid (MM), the maximum cycle temperature is set to 200 °C, which is lower than its critical temperature. Therefore, the cycle will be operated as subcritical ORC for both Design 1 and Design 2.

The following Table 3 introduces other design bases for Case Study 1 on Biogas ICE WHR ORC systems. The main aspects covered include system basis, ambient conditions, rotating equipment, heat exchangers definition, and the optimization set-up. The main values that change from Design 1 to Design 2 are highlighted in grey. Those are mainly related to the rig limitation that imposes limitations in attainable working fluid pressure at the inlet of the expander, leading to a subcritical cycle. In this work, Case Study 1 is assumed to have the same Design 1 and Design 2 conditions as Case study 3 due to the similar operating conditions.

[2] https://agrikomp.com/utilisation/biogas-chp/

Table 3. Design basis for Case Study 1 on Biogas ICE WHR ORC systems.

Item		Unit	SINTEF	
			Design 1	Design 2
1. System basis		-		
	Process configuration	-	simple or recuperated	simple or recuperated
	Working fluid		MM	MM
	Operating condition	-	subcritical only	subcritical only
1.1 Heat source				
	Fluid	-	flue gas	flue gas
	Mass flow rate	kg/s	0.290	0.290
	Evaporator inlet p	bara	1.01325	1.01325
	Heat source pump/fan outlet p	bara	1.01325	1.01325
	Evaporator inlet T(= $T_{evap,out,max}$)	°C	580	580
	Minimum evaporator outlet T	°C	160	130
1.2 Heat sink				
	Fluid	-	cooling water	cooling water
	Mass flow rate	kg/s	var	var
	Heat sink pump inlet p	bara	1.01325	1.01325
	Condenser outlet p	bara	1.01325	1.01325
	Condenser inlet T(= $T_{cond,out,min}$)	°C	17	17
	Maximum condenser outlet T	°C	27	27
2. Ambient condition				
2.1 Air				
	Temperature	°C	17	17
	Pressure	bara	1.01325	1.01325
3. Rotating Equipment				
3.1 Pump				
	Minimum inlet subcooling	°C	9.6	5
	Isentropic efficiency	%	75	75
3.2 Fan				
	Isentropic efficiency	%	85	85
3.3 Expander				
	Maximum inlet T	°C	190	200
	Minimum inlet superheating	°C	10	2
	Maximum inlet p	bara	8	10
	Minimum outlet p	bara	0.2	0.12
	Maximum power output	kWe	50	50
	Isentropic efficiency	%	65	70
4. Heat exchangers				
4.1 ΔTmin				
	Evaporator	°C	50	20

Condenser	°C	2	1
Recuperator	°C	20	20
4.2 Δp			
Gas side in evaporator/in others	% of inlet	0.25 / 5	0.25 / 5
Liquid side	% of inlet	5	5
5. Optimization			
5.1 objective function			
Net power output	-	Y	Y
5.2 variables			
Heat source exit temperature	-	Y	Y
Heat sink exit temperature	-	Y	Y
Pump inlet pressure	-	Y	Y
Pump inlet enthalpy	-	Y	Y
Expander inlet pressure	-	Y	Y
Expander inlet enthalpy	-	Y	Y
Recuperator effectiveness	-	(Y)	(Y)

3.2.2 Case Study 2: Low temperature geothermal ORC

Case Study 2 does not consider heat production from low temperature geothermal heat source. Thus, cooling water is selected as a heat sink. Since the maximum working fluid temperature (or maximum expander inlet temperature) is set to 150 °C, which is lower than the critical temperature, the ORC system under Design 1 and Design 2 will be operated at subcritical condition.

The following Table 4 summarizes the design basis for Case Study 2 on Low temperature geothermal ORC systems using deep energy wells. The main aspects covered include system basis, ambient conditions, rotating equipment, heat exchangers definition and the optimization set-up. The main values that change from Design 1 to Design 2 are highlighted in grey. Those are mainly related to the rig limitation that imposes limitations in attainable working fluid pressure at the inlet of the expander, leading to subcritical or trans-critical cycles.

Table 4. Design basis for Case Study 2 on Low temperature geothermal ORC systems using deep energy wells.

Item	Unit	NTNU	
		Design 1	Design 2
1. System basis	-		
Process configuration	-	simple or recuperated	simple or recuperated
Working fluid		r600a	r600a
Operating condition	-	subcritical only	subcritical only
1.1 Heat source			
Fluid	-	steam	steam
Mass flow rate	kg/s	2.5	2.5

	Evaporator inlet p	bara	3	3
	Heat source pump/fan outlet p	bara	3	3
	Evaporator inlet T(=$T_{evap,out,max}$)	°C	120	120
	Minimum evaporator outlet T	°C	75	75
1.2 Heat sink				
	Fluid	-	cooling water	cooling water
	Mass flow rate	kg/s	var	var
	Heat sink pump inlet p	bara	1.01325	1.01325
	Condenser outlet p	bara	1.01325	1.01325
	Condenser inlet T(=$T_{cond,out,min}$)	°C	10	10
	Maximum condenser outlet T	°C	20	20
2. Ambient condition				
2.1 Air				
	Temperature	°C	10	10
	Pressure	bara	1.01325	1.01325
2.2 Water				
	Temperature	°C	10	10
	Pressure	bara	1.01325	1.01325
3. Rotating Equipment				
3.1 Pump				
	Minimum inlet subcooling	°C	5	1
	Isentropic efficiency	%	70	70
3.2 Fan				
	Isentropic efficiency	%	-	-
	Motor efficiency	%	-	-
	Mechanical efficiency	%	-	-
3.3 Expander				
	Maximum inlet T	°C	150	150
	Minimum inlet superheating	°C	5	2
	Maximum inlet p	bara	12	50
	Minimum outlet p	bara	1.5	0.5
	Maximum power output	kWe	50	50
	Isentropic efficiency	%	70	70
4. Heat exchangers				
4.1 ΔTmin				
	Evaporator	°C	10	5
	Condenser	°C	10	5
	Recuperator	°C	10	5
4.2 Δp				
	Gas side	% of inlet	2	2
	Liquid side	% of inlet	2	2
5. Optimization				
5.1 objective function				

	Net power output	-	Y	Y
5.2 variables				
	Heat source exit temperature	-	Y	Y
	Heat sink exit temperature	-	Y	Y
	Pump inlet pressure	-	Y	Y
	Pump inlet enthalpy	-	Y	Y
	Expander inlet pressure	-	Y	Y
	Expander inlet enthalpy	-	Y	Y
	Recuperator effectiveness	-	(Y)	(Y)

3.2.3 Case Study 3: Biomass micro-CHP ORC

Flue gas conditions are estimated based on the fuel composition and excess air-fuel ratio supplied from CTU (Table 5 and Table 6). In order to have a good match of enthalpy changes between the estimated flue gas and the actual flue gas, the mass flow rate of the estimated flue gas is revised from the actual flue gas value (see Appendix A.3 Case study 3).

Table 5. Fuel composition (Woodchips 20 %W) (from CTU).

Compostion	Fraction
C	0.5096
H	0.0693
O	0.4183
N	0.0026

Table 6. Flue gas enthalpy table with excess air-fuel ratio of 1.8 (from CTU).

Temperature [°C]	H_{fg} [kJ/kg_fg]
0	0
25	32.2
100	128.8
200	260.4
300	395.3
400	533.7
500	675.8
600	821.5
700	970.5
800	1122.6
900	1277.6
1000	1435.5
1100	1595.4
1200	1757.4
1300	1920.8

Table 7. Estimated flue gas composition and mass flow rate.

Item	Unit	Value
Actual flue gas mass flow	kg/s	0.078
Mass correction factor	-	1.234
Estimated flue gas mass flow	kg/s	0.096
Estimated flue gas composition		
CO_2	mol%	9.852
H_2O	mol%	7.983
N_2	mol%	73.483
O_2	mol%	8.682

In consideration with heat production for local usage, heating water is selected as a heat sink for Case Study 3. The maximum cycle temperature is also set to 200 °C to avoid the degradation of the working fluid (MM), which is lower than its critical temperature. Therefore, the cycle will be operated as subcritical ORC for both Design 1 and Design 2.

The following Table 8 summarizes other design conditions for Case Study 3 on micro-CHP ORC systems. The main aspects covered include system basis, ambient conditions, rotating equipment, heat exchangers definition and the optimization set-up. The main values that change from Design 1 to Design 2 are highlighted in grey. Those are mainly related to the rig limitation that imposes limitations in attainable working fluid pressure at the inlet of the expander, leading to subcritical or trans-critical cycles.

Table 8. Design basis for Case Study 3 on biomass micro-CHP ORC systems.

Item		Unit	CTU	
			Design 1	Design 2
1. System basis		-		
	Process configuration	-	simple or recuperated	simple or recuperated
	Working fluid		MM	MM
	Operating condition	-	subcritical only	subcritical only
1.1 Heat source				
	Fluid	-	flue gas	flue gas
	Mass flow rate	kg/s	0.078	0.078
	Evaporator inlet p	bara	1.01325	1.01325
	Heat source pump/fan outlet p	bara	1.01325	1.01325
	Evaporator inlet T (=$T_{evap,out,max}$)	°C	944	944
	Minimum evaporator outlet T	°C	132	100
1.2 Heat sink				
	Fluid	-	water	water
	Mass flow rate	kg/s	var (nominal 1.136)	var (nominal 1.136)

	Heat sink pump inlet p	bara	2.1	2.1
	Condenser outlet p	bara	2	2
	Condenser inlet T(=$T_{cond,out,min}$)	°C	58	58
	Maximum condenser outlet T	°C	85	85
2. Ambient condition				
2.1 Air				
	Temperature	°C	7	7
	Pressure	bara	1.01325	1.01325
3. Rotating Equipment				
3.1 Pump				
	Minimum inlet subcooling	°C	9.6	5
	Isentropic efficiency	%	75	75
3.2 Fan				
	Isentropic efficiency	%	85	85
3.3 Expander				
	Maximum inlet T	°C	190	200
	Minimum inlet superheating	°C	10	2
	Maximum inlet p	bara	8	10
	minimum outlet p	bara	0.2	0.12
	Maximum power output	kWe	15.5	50
	Isentropic efficiency	%	55.05	70
4. Heat exchangers				
4.1 ΔTmin				
	Evaporator	°C	50	20
	Condenser	°C	2	1
	Recuperator	°C	20	20
4.2 Δp				
	Gas side in evaporator/in others	% of inlet	0.25 / 5	0.25 / 5
	Liquid side	% of inlet	5	5
5. Optimization				
5.1 objective function				
	Net power output	-	Y	Y
5.2 variables				
	Heat source exit temperature	-	Y	Y
	Heat sink exit temperature	-	Y	Y
	Pump inlet pressure	-	Y	Y
	Pump inlet enthalpy	-	Y	Y
	Expander inlet pressure	-	Y	Y
	Expander inlet enthalpy	-	Y	Y
	Recuperator effectiveness	-	(Y)	(Y)

3.3 Modelling and optimization

The Rankine Lab[3] tool has been used as model basis for optimization (see Figure 5 for an illustration of the process flowsheet and of the optimization workflow). It is a MATLAB tool that can be used to analyze and optimize Rankine cycles. It utilizes a gradient based optimizer (SQP), and several cycle configurations are possible to analyze. In addition, several working fluids can be chosen, being linked to RefProp and CoolProp. Several parameters can be tuned to perform a simulation.

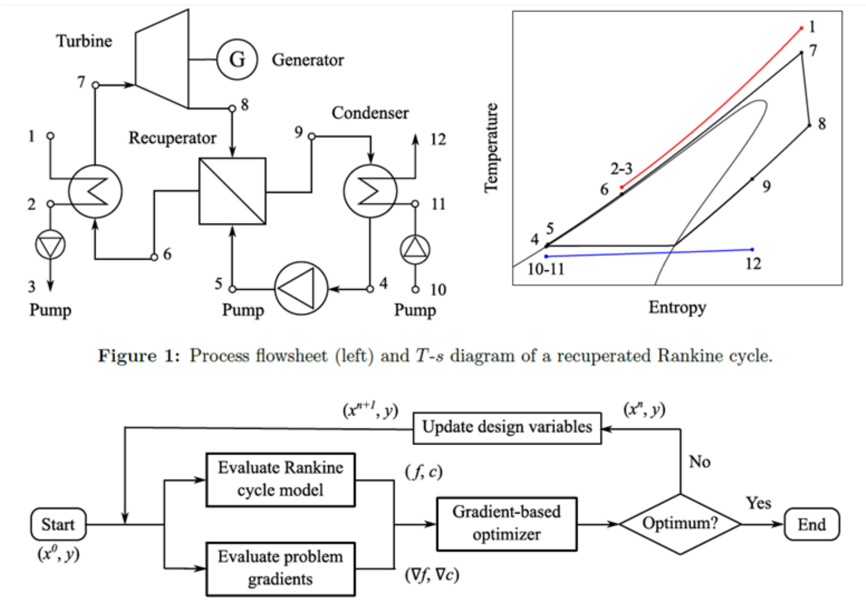

Figure 5. Rankine Lab tool for Rankine cycle optimization.

For the optimization of the ORC systems, 7 decision variables and 9 inequality constraints are defined as shown in Table 9 and Table 10. The upper and lower bounds of the variables defined in Table 9 (such as minimum heat source exit temperature) are given in Chapter 3.2. The values for the constraints are also indicated in the design basis (see Table 3, Table 4, and Table 8).

Table 9. Formulation of independent variables.

Independent variables	Unit	Value
Heat source exit temperature	K	$T_{3,min} < T_3 < T_{3,max}$
Heat sink exit temperature	K	$T_{12,min} < T_{12} < T_{12,max}$
Pump inlet pressure*	Pa	$p_{min} < p_4 < p_{max}$
Pump inlet enthalpy**	J/kg	$h_{min} < h_4 < h_{max}$
Expander inlet pressure*	Pa	$p_{min} < p_7 < p_{max}$
Expander inlet enthalpy**	J/kg	$h_{min} < h_7 < h_{max}$
Recuperator effectiveness***	-	$0 \leq \varepsilon_{rec} = \dfrac{h_6 - h_5}{h(p_6, T_8) - h_5} \leq 1$

* Using $p_{min} = p_{triple}$ and p_{max} = 20 bara for Case Study 1 and 3 or 50 bara for Case Study 2.
** Using $h_{min} = h_{sat}(T_0)$ and $h_{max} = h(T_1, p \to 0)$.
** For Case study 1 and 3, $h_{max} = h(1000\ K, p \to 0)$ since the thermo package can handle MM until 1000K.
*** The model reduces to a simple cycle architecture when $\varepsilon_{rec} = 0$.

[3] For the open code and technical documentation, refer to https://github.com/RoberAgro/RankineLab

Table 10. Formulation of nonlinear constraints.

Nonlinear constraints	Unit	Value
ΔT within the evaporator*	K	$\Delta T_{evap} \geq \Delta T_{evap,min}$
ΔT within the recuperator*	K	$\Delta T_{rec} \geq \Delta T_{rec,min}$
ΔT within the condenser*	Pa	$\Delta T_{cond} \geq \Delta T_{cond,min}$
Subcooling at the pump inlet	K	$\Delta T_{sub,min} \leq T_{sat}(p_4) - T_4 \leq \Delta T_{sub,max}$
Superheating at the expander inlet	K	$\Delta T_{sup,min} \leq T_7 - T_{sat}(p_7) \leq \Delta T_{sup,max}$
Vapor quality within the expander	-	$q_{exp} \geq q_{exp,min}$
Expander capacity	W	$P_{exp} \leq P_{exp,max}$
Expander inlet temperature	K	$T_7 \leq T_{exp,in,max}$
Expander outlet pressure	Pa	$T_8 \geq T_{exp,out,min}$

* This constraint is evaluated at each of the discretization of the heat exchanger.

The objective function selected to identify the optimal solution was the *net power output*. This was deemed as the most appropriate metric for this kind of distributed application where effectiveness needs to be conjugated with ease of implementation and compactness. Other KPIs presented in results section are defined as:

Plant efficiency: $$\frac{w_{net}}{Q_{max}} \tag{1}$$

Cycle efficiency: $$\frac{w_{net}}{Q_{eva}} \tag{2}$$

Plant exergy efficiency: $$\frac{w_{net}}{Exh_{in}} \tag{3}$$

Cycle exergy efficiency: $$\frac{w_{net}}{Ex_{eva}} \tag{4}$$

where the following terms are considered:

- w_{net}: net power output
- Q_{max}: heat available in the heat source
- Q_{eva}: heat extracted by the evaporator
- EX_{hin}: exergy available in the heat source
- EX_{eva}: exergy extracted by the evaporator

In order to give preliminary indication of expander design, the speed and the diameter of the turbomachinery are also estimated by considering the specific speed (ω_s) and the specific diameter (d_s)[4].

$$\omega_s = \omega(\dot{m}\rho_{8s})^{\frac{1}{2}}/(h_7 - h_{8s})^{\frac{3}{4}} \tag{5}$$

$$d_s = d(h_7 - h_{8s})^{\frac{1}{4}}/(\dot{m}/\rho_{8s})^{\frac{1}{2}} \tag{6}$$

where ω is the actual angular velocity, $\dot{m}$ is the mass flow rate, ρ is the fluid density, h is the specific enthalpy, d is the rotor diameter. The subscript $_s$ means isentropic states (i.e., $h_{8s} = h(p_8, s_7)$ and $\rho_{8s} = \rho(p_8, s_7)$). As a rule of thumb, it is assumed that $\omega_s \times d_s = 2$ and $\omega_s = 0.5$ for the calculation of ω and d.

[4] S. L. Dixon & C. A. Hall, Fluid Mechanics and Thermodynamics of Turbomachinery (Sixth Edition). Boston: Butterworth-Heinemann.

4 Results

4.1 Case Study 1: Biogas

Four optimization runs have been performed for Case Study 1:

- Design 1
- Design 1 with recuperator
- Design 2
- Design 2 with recuperator

and Figure 6 shows the temperature-enthalpy diagrams of the optimal operating conditions. The detailed stream conditions are included at the end of this chapter (Table 13). The values of the variables and constraints from the optimal solutions are also shown in Appendix A.1.

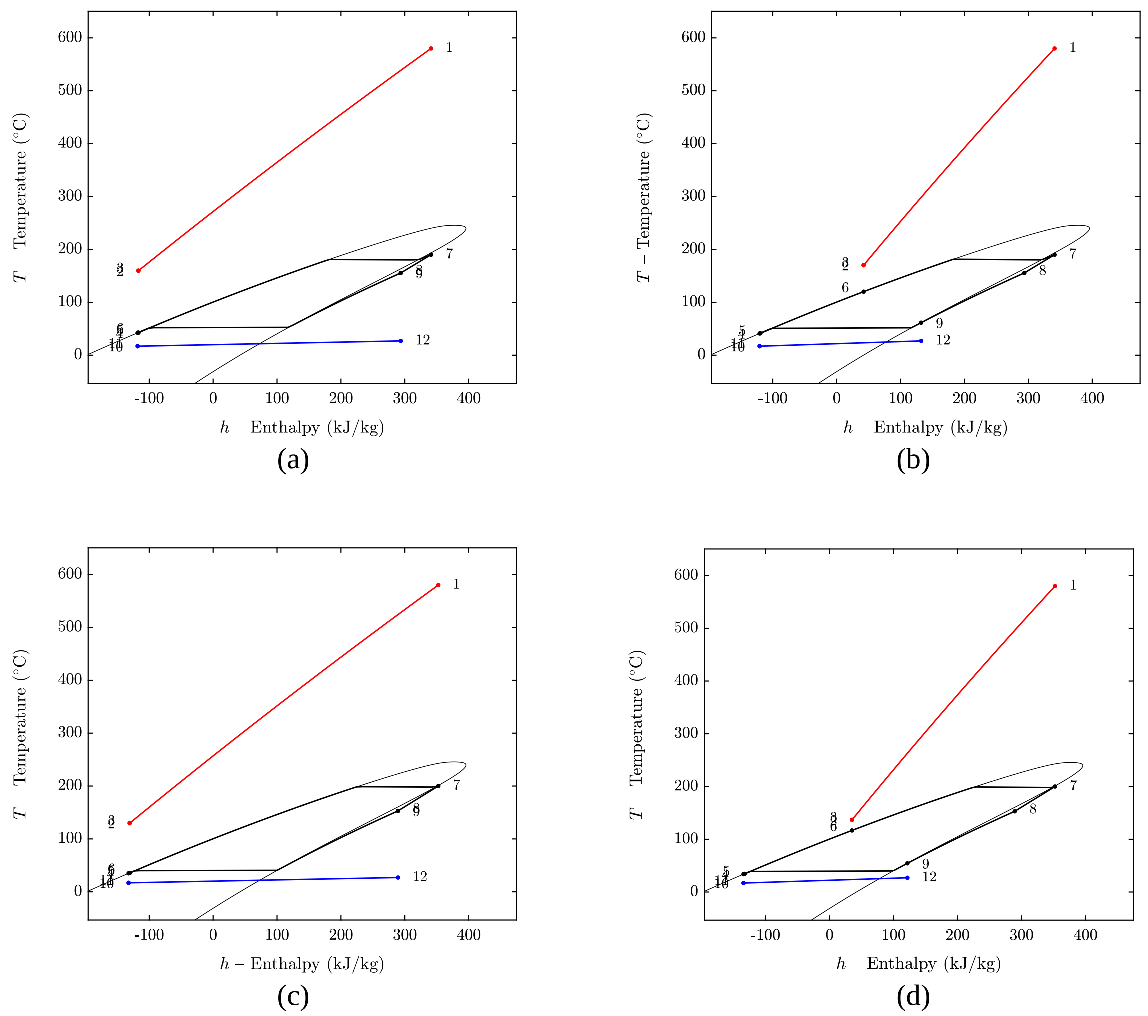

Figure 6. Temperature-enthalpy diagram of optimized Case study 1. (a) Design 1, (b) Design 1 with recuperator, (c) Design 2, (d) Design 2 with recuperator.

Table 11. System performance of optimized Case Study 1.

Parameter	Unit	design 1	design 1 rec	design 2	design 2 rec
W_exp	kW	14.58	21.81	19.64	29.45
W_pump_h	kW	0.11	0.11	0.10	0.10
W_pump_f	kW	0.36	0.57	0.51	0.81
W_pump_c	kW	0.02	0.02	0.02	0.02
W_net	kW	14.08	21.11	19.01	28.52
eta_plant_energy	%	6.03	9.03	8.13	12.21
eta_cycle_energy	%	9.98	15.32	12.63	19.23
eta_plant_exergy	%	16.19	24.26	21.84	32.78
eta_cycle_exergy	%	18.66	28.40	24.26	36.70

Table 11 shows the comparison in terms of efficiency for each of Design 1 and 2, with and without a recuperator. The optimal solution of Design 2 with a recuperator gives the highest energy and exergy efficiency. It is worth noting that considering the quality of heat collected from the heat source, the exergy efficiencies tend to have a higher value than energy based efficiencies. As seen in Table 11, not restricting the design to rig constraints provides higher efficiency in the optimized thermodynamic cycle design. In addition, including a recuperator in the cycle configuration increases the plant and cycle efficiency. Design 1 with recuperator even gives a larger net power production and a higher efficiency than Design 2 where the ORC system is operated under practical limits.

Table 12. Expander parameters for optimized Case Study 1.

Parameter	Unit	design 1	design 1 rec	design 2	design 2 rec
Isentropic efficiency	-	0.65	0.65	0.70	0.70
Power output	kW	14.58	21.81	19.64	29.45
Pressure ratio	-	32.10	32.10	74.10	74.10
Diameter	cm	13.87	16.96	17.04	20.86
RPM	rpm	37162.84	30379.16	33639.38	27471.07
T_{exp_in}	°C	190 (max 190)	190 (max 190)	200 (max 200)	200 (max 200)
p_{exp_in}	bara	6.4 (max 8)	6.4 (max 8)	8.9 (max 10)	8.9 (max 10)
p_{exp_out}	bara	0.2 (min 0.2)	0.2 (min 0.2)	0.12 (min 0.12)	0.12 (min 0.12)

The results from the thermodynamic optimization and resulting expander design parameters are presented in Table 12. The power output of the expander in Case Study 1 is ranged from around 15 to 30 kW. The expander has a high pressure ratio for both Design 1 and 2 due to the low expander outlet pressure level. Preliminary estimation of expander design with the thermodynamic optima of the ORC system gives the diameter from ca. 14 to 21 cm and the RPM ca. from 30000 to 38000, which are acceptable values for small-scale expanders. For all cases, the expander inlet temperature reaches the upper limit, indicating that increasing turbine inlet temperature is the key factor for further improvement of the ORC system.

The resulting heat duty, LMTD, and size (UA) of the evaporator, condenser, and recuperator are presented in Figure 7. For all cases, the heat duty of the evaporator and the condenser are at a similar level for this case study. However, due to the high temperature heat source (biogas combustion flue gas), the LMTD in the evaporator is significantly larger than other heat exchangers, giving a smaller UA value. It is worth noting that although the recuperator increases the power production, the size (UA) of the recuperator could be considerably larger than the evaporator when it is in use. Thus, the economic benefit of a recuperator in the ORC system needs to be verified in consideration of the additional capital cost.

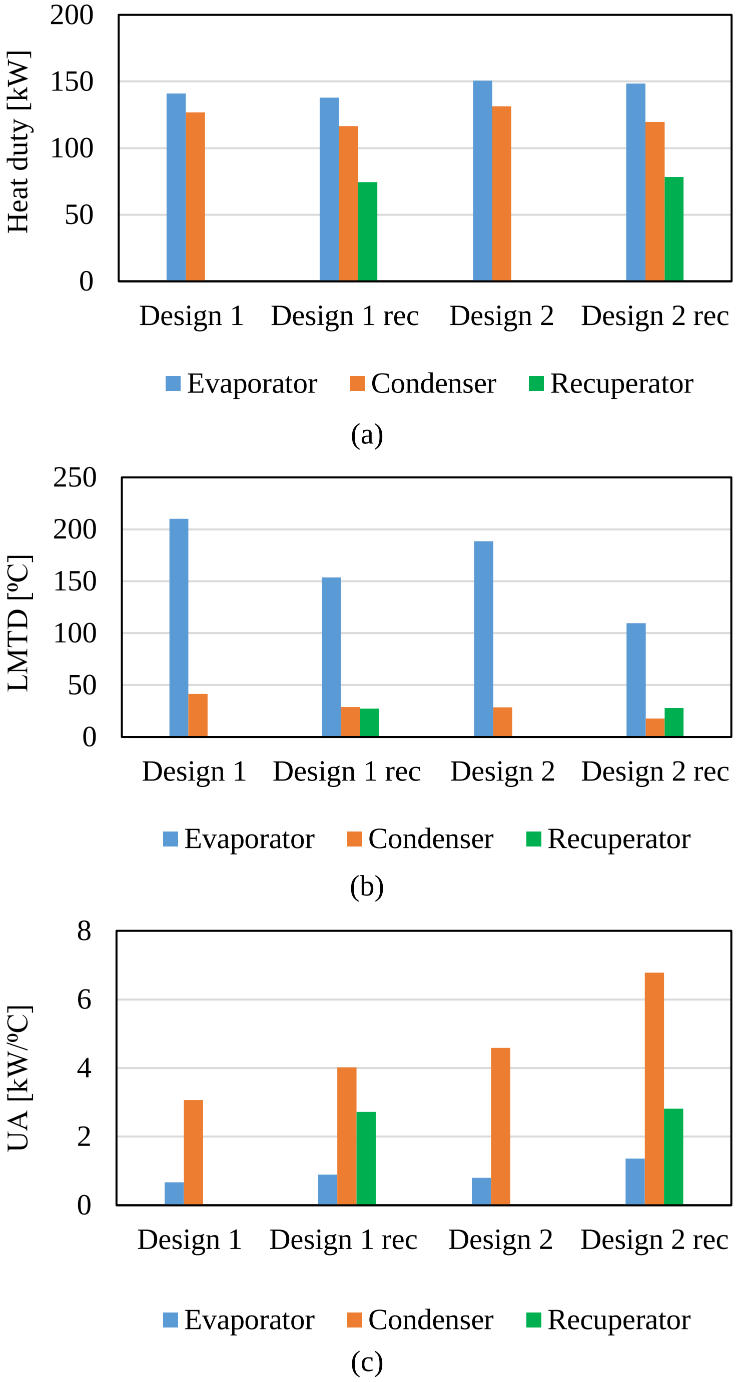

Figure 7. Heat exchanger parameters for optimized Case Study 1. (a) Heat duty, (b) LMTD, (c) UA.

Table 13 Stream conditions for optimized Case study 1.

Stream	fluid* [-]	m [kg/s]	p [Pa]	T [K]	d [kg/m3]	h [J/kg]	s [J/kg/K]	e [J/kg]
Design 1								
1	'REFPROP::flue gas'	0.2897	101325.0	853.2	0.4141	1151240.3	7487.5	300334.8
2	'REFPROP::flue gas'	0.2897	101070.0	432.8	0.8146	664357.1	6707.1	39878.7
3	'REFPROP::flue gas'	0.2897	101325.0	433.2	0.8160	664725.0	6707.2	40209.7
4	'HEOS::MM'	0.3080	19000.0	315.5	741.0536	-118108.2	-342.9	1900.4
5	'HEOS::MM'	0.3080	675876.2	315.8	741.8756	-116927.2	-341.9	2810.1
6	'HEOS::MM'	0.3080	675876.2	315.8	741.8756	-116927.2	-341.9	2810.1
7	'HEOS::MM'	0.3080	642082.4	463.2	34.3865	341101.5	788.6	132822.3
8	'HEOS::MM'	0.3080	20000.0	428.7	0.9178	293771.2	849.0	67956.1
9	'HEOS::MM'	0.3080	20000.0	428.7	0.9178	293771.2	849.0	67956.1
10	'HEOS::Water'	3.0330	101325.0	290.2	998.7780	71451.7	253.4	0.0
11	'HEOS::Water'	3.0330	106657.9	290.2	998.7804	71458.8	253.4	5.3
12	'HEOS::Water'	3.0330	101325.0	300.2	996.5158	113282.0	395.2	704.5
Design 1 with recuperator								
1	'REFPROP::flue gas'	0.2897	101325.0	853.2	0.4141	1151240.3	7487.5	300334.8
2	'REFPROP::flue gas'	0.2897	101070.0	443.2	0.7954	675768.7	6733.1	43730.8
3	'REFPROP::flue gas'	0.2897	101325.0	443.6	0.7968	676145.5	6733.3	44070.7
4	'HEOS::MM'	0.4609	18050.0	314.2	742.3984	-120536.3	-350.6	1708.8
5	'HEOS::MM'	0.4609	711448.6	314.6	743.2552	-119291.9	-349.6	2666.2
6	'HEOS::MM'	0.4609	675876.2	393.2	652.4090	42201.4	107.8	31448.6
7	'HEOS::MM'	0.4609	642082.4	463.2	34.3865	341101.5	788.6	132822.3
8	'HEOS::MM'	0.4609	20000.0	428.7	0.9178	293771.2	849.0	67956.1
9	'HEOS::MM'	0.4609	19000.0	334.6	1.1284	132277.9	427.6	28735.5
10	'HEOS::Water'	2.7859	101325.0	290.2	998.7780	71451.7	253.4	0.0
11	'HEOS::Water'	2.7859	106657.9	290.2	998.7804	71458.8	253.4	5.3
12	'HEOS::Water'	2.7859	101325.0	300.2	996.5158	113282.0	395.2	704.5
Design 2								
1	'REFPROP::flue gas'	0.2897	101325.0	853.2	0.4141	1151240.3	7487.5	300334.8
2	'REFPROP::flue gas'	0.2897	101070.0	402.8	0.8753	631659.6	6628.8	29896.2
3	'REFPROP::flue gas'	0.2897	101325.0	403.2	0.8769	632002.1	6628.9	30201.6
4	'HEOS::MM'	0.3117	11400.0	308.1	748.9069	-132295.1	-388.3	906.0
5	'HEOS::MM'	0.3117	936029.9	308.6	749.9814	-130650.3	-387.0	2164.1
6	'HEOS::MM'	0.3117	936029.9	308.6	749.9814	-130650.3	-387.0	2164.1
7	'HEOS::MM'	0.3117	889228.4	473.2	52.0794	352365.5	800.2	140725.1
8	'HEOS::MM'	0.3117	12000.0	426.2	0.5524	289345.6	864.7	58988.8
9	'HEOS::MM'	0.3117	12000.0	426.2	0.5524	289345.6	864.7	58988.8
10	'HEOS::Water'	3.1419	101325.0	290.2	998.7780	71451.7	253.4	0.0
11	'HEOS::Water'	3.1419	106657.9	290.2	998.7804	71458.8	253.4	5.3
12	'HEOS::Water'	3.1419	101325.0	300.2	996.5158	113282.0	395.2	704.5
Design 2 with recuperator								
1	'REFPROP::flue gas'	0.2897	101325.0	853.2	0.4141	1151240.3	7487.5	300334.8
2	'REFPROP::flue gas'	0.2897	101070.0	409.8	0.8603	639285.3	6647.6	32076.5
3	'REFPROP::flue gas'	0.2897	101325.0	410.2	0.8618	639633.7	6647.7	32388.0
4	'HEOS::MM'	0.4673	10830.0	307.0	750.1210	-134485.3	-395.4	781.2
5	'HEOS::MM'	0.4673	985294.6	307.5	751.2404	-132754.8	-394.0	2103.4
6	'HEOS::MM'	0.4673	936029.9	389.8	657.6763	34974.1	88.3	29871.5
7	'HEOS::MM'	0.4673	889228.4	473.2	52.0794	352365.5	800.2	140725.1
8	'HEOS::MM'	0.4673	12000.0	426.2	0.5524	289345.6	864.7	58988.8
9	'HEOS::MM'	0.4673	11400.0	327.5	0.6874	121616.7	421.2	19935.3
10	'HEOS::Water'	2.8616	101325.0	290.2	998.7780	71451.7	253.4	0.0
11	'HEOS::Water'	2.8616	106657.9	290.2	998.7804	71458.8	253.4	5.3
12	'HEOS::Water'	2.8616	101325.0	300.2	996.5158	113282.0	395.2	704.5

4.2 Case Study 2: Geothermal

Four optimization runs have been performed for Case Study 2:

- Design 1
- Design 1 with recuperator
- Design 2
- Design 2 with recuperator

and Figure 8 shows the temperature-enthalpy diagrams of the optimal operating conditions. The detailed stream conditions are included at the end of this chapter (Table 16). The values of the variables and constraints from the optimal solutions are also shown in Appendix A.2.

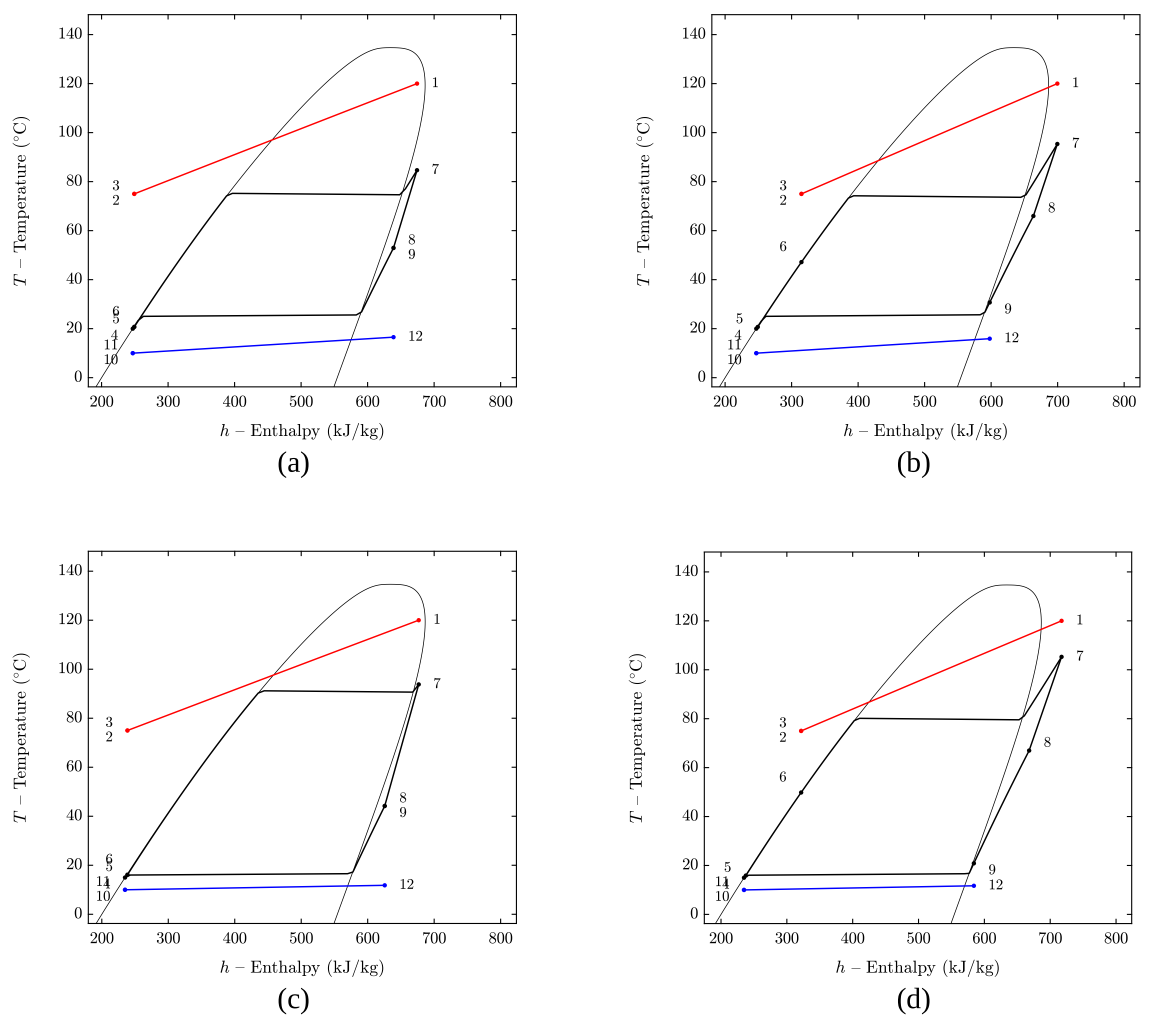

Figure 8. Temperature-enthalpy diagram of optimized Case study 2. (a) Design 1, (b) Design 1 with recuperator, (c) Design 2, (d) Design 2 with recuperator.

Table 14. System performance of Case Study 2.

Parameter	Unit	design 1	design 1 rec	design 2	design 2 rec
W_exp	kW	31.55	35.50	44.27	47.22
W_pump_h	kW	0.02	0.02	0.02	0.02
W_pump_f	kW	2.00	2.20	3.13	2.71
W_pump_c	kW	0.04	0.04	0.13	0.14
W_net	kW	29.50	33.25	40.98	44.35
eta_plant_energy	%	3.19	3.60	4.44	4.80
eta_cycle_energy	%	7.78	8.77	10.80	11.69
eta_plant_exergy	%	20.50	23.11	28.48	30.83
eta_cycle_exergy	%	33.06	37.26	45.93	49.70

Table 14 shows the comparison in terms of efficiency for each of Design 1 and 2, with and without a recuperator. The optimal solution of Design 2 with a recuperator gives the highest energy and exergy efficiency. It is worth noting that considering the quality of heat collected from the heat source, the exergy efficiencies tend to have a significantly higher value than energy based efficiencies. In this case study, Design 2 provides higher energy and exergy efficiency in the optimized thermodynamic cycle design compared to Design 1. The use of a recuperator in the cycle also increases the plant and cycle efficiency.

Table 15. Expander parameters for optimized Case Study 2.

Parameter	Unit	design 1	design 1 rec	design 2	design 2 rec
Isentropic efficiency	-	0.70	0.70	0.70	0.70
Power output	kW	31.55	35.50	44.27	47.22
Pressure ratio	-	3.35	3.21	6.10	4.77
Diameter	cm	8.62	9.15	8.74	9.62
RPM	rpm	49814.61	47324.91	59070.63	52658.43
T_{exp_in}	°C	84.7 (max 110)*	95.4 (max 110)*	93.8 (max 115)*	105.3 (max 115)*
p_{exp_in}	bara	12 (max 12)	11.7 (max 12)	16.6 (max 50)	13.3 (max 50)
p_{exp_out}	bara	3.5 (min 1.5)	3.7 (min 1.5)	2.7 (min 1.5)	2.8 (min 1.5)

* TiT max is 150 °C but heat source inlet T-dTmin = 110 °C for Design 1 and 115 °C for Design 2.

The results from the thermodynamic optimization and resulting expander design parameters are presented in Table 15. The power output of the expander in Case Study 2 is ranged from around 30 to 50 kW. The expander has a low pressure ratio for both Design 1 and 2 due to the high expander outlet pressure level. Preliminary estimation of expander design gives the diameter from ca. 9 to 10 cm and the RPM ca. from 47000 to 60000, which are acceptable values for small-scale expanders. For all cases, the expander inlet temperature does not reach the upper limit although a higher turbine inlet temperature (TiT) typically results in increased expander power and efficiency. In Case Study 2, if the TiT is increased to the upper limit, the optimal solution of the ORC system gives a lower net power production. From the optimal solutions, it is shown that with a given heat input (or enthalpy difference of the working fluid through the condenser), the condenser outlet temperature of the working fluid (=TiT) is increased by reducing the mass flow rate and lowering the pressure level, resulting in lower pressure ratio and power output of the expander. If, however, there is a sufficient heat input to the condenser, the TiT and the net power production will increase as seen in Design 2 with a recuperator.

Assuming a simple configuration, **the expander design parameters for further consideration in WP2 should be the ones for Design 1**, representing boundary conditions and design parameters for a simple ORC cycle with isobutane as working fluid, and considering the expander rig constraints at the NTNU Expand test rig.

The resulting heat duty, LMTD, and size (UA) of the evaporator, condenser, and recuperator are presented in Figure 9. For all cases, the heat duty of the evaporator and the condenser are at a similar level for this case study. However, due to the smaller LMTD, the evaporator has a significantly larger UA value than other heat exchangers. It is worth noting that although the recuperator increases the power production, the size of the recuperator could be significantly larger than the evaporator when it is in use. Thus, the economic benefit of a recuperator in the ORC system needs to be verified in consideration of the additional capital cost.

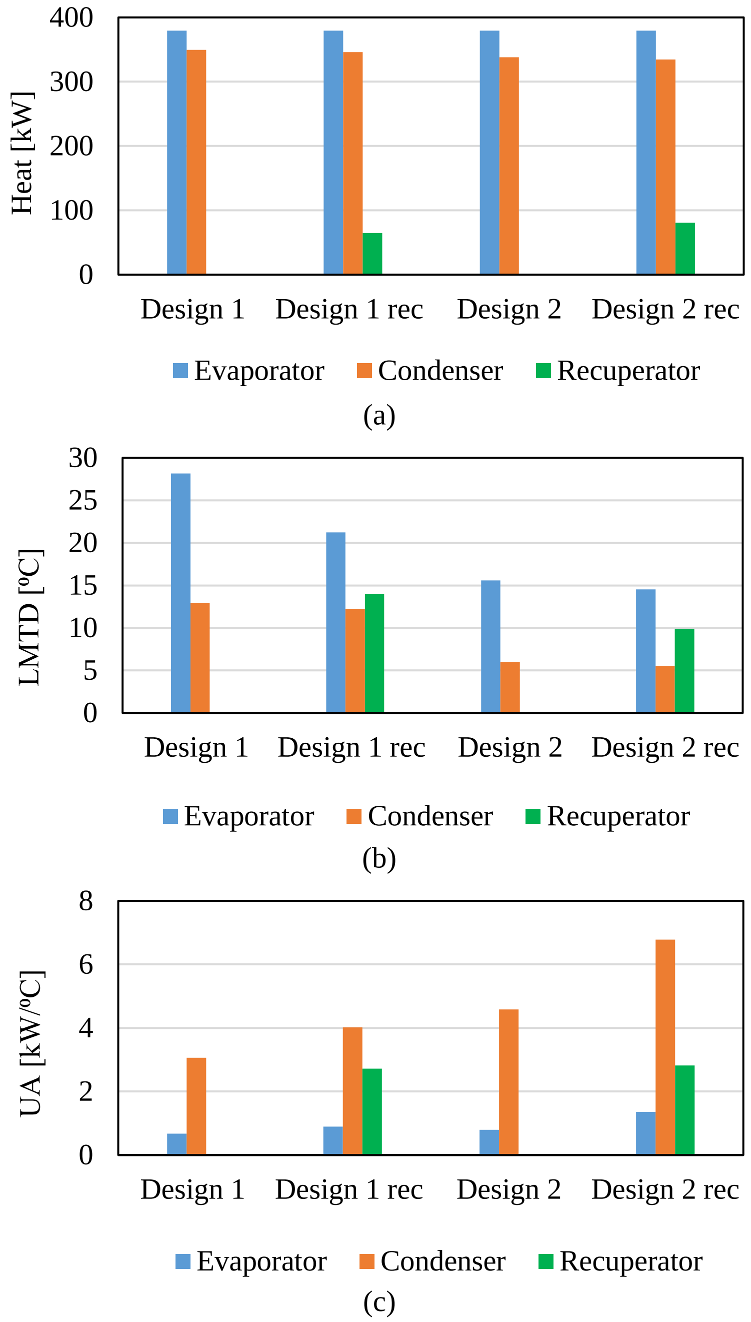

Figure 9. Heat exchanger parameters for optimized Case Study 2. (a) Heat duty, (b) LMTD, (c) UA.

Table 16 Stream conditions for optimized Case study 2.

Stream	fluid* [-]	m [kg/s]	p [Pa]	T [K]	d [kg/m3]	h [J/kg]	s [J/kg/K]	e [J/kg]
Design 1								
1	'HEOS::Water'	2.0000	300000.0	393.2	943.1574	503882.9	1527.8	71940.4
2	'HEOS::Water'	2.0000	294000.0	348.1	974.9291	314232.1	1015.6	27325.5
3	'HEOS::Water'	2.0000	300000.0	348.2	974.9312	314240.9	1015.6	27332.2
4	'HEOS::Isobutane'	0.8922	350671.9	293.2	556.9557	246911.6	1164.5	30621.1
5	'HEOS::Isobutane'	0.8922	1224489.8	293.9	557.8101	249150.5	1166.8	32212.5
6	'HEOS::Isobutane'	0.8922	1224489.8	293.9	557.8101	249150.5	1166.8	32212.5
7	'HEOS::Isobutane'	0.8922	1200000.0	357.8	29.5524	674298.6	2422.4	101843.1
8	'HEOS::Isobutane'	0.8922	357828.5	326.1	8.2774	638933.3	2469.4	53151.2
9	'HEOS::Isobutane'	0.8922	357828.5	326.1	8.2774	638933.3	2469.4	53151.2
10	'HEOS::Water'	12.7843	101325.0	283.2	999.7025	42118.9	151.1	0.0
11	'HEOS::Water'	12.7843	103392.9	283.2	999.7034	42121.9	151.1	2.1
12	'HEOS::Water'	12.7843	101325.0	289.7	998.8586	69479.5	246.6	310.6
Design 1 with recuperator								
1	'HEOS::Water'	2.0000	300000.0	393.2	943.1574	503882.9	1527.8	71940.4
2	'HEOS::Water'	2.0000	294000.0	348.1	974.9291	314232.1	1015.6	27325.5
3	'HEOS::Water'	2.0000	300000.0	348.2	974.9312	314240.9	1015.6	27332.2
4	'HEOS::Isobutane'	0.9858	350671.9	293.2	556.9557	246911.6	1164.5	30621.1
5	'HEOS::Isobutane'	0.9858	1220182.3	293.9	557.8059	249139.5	1166.8	32204.7
6	'HEOS::Isobutane'	0.9858	1195778.7	320.3	523.0276	314790.2	1380.7	37274.5
7	'HEOS::Isobutane'	0.9858	1171863.1	368.5	27.0155	699543.2	2494.6	106625.5
8	'HEOS::Isobutane'	0.9858	365131.1	339.1	8.0527	663529.3	2540.7	57569.3
9	'HEOS::Isobutane'	0.9858	357828.5	303.9	9.0910	597878.6	2339.1	49010.4
10	'HEOS::Water'	13.9772	101325.0	283.2	999.7025	42118.9	151.1	0.0
11	'HEOS::Water'	13.9772	103392.9	283.2	999.7034	42121.9	151.1	2.1
12	'HEOS::Water'	13.9772	101325.0	289.1	998.9611	66876.1	237.6	254.6
Design 2								
1	'HEOS::Water'	2.0000	300000.0	393.2	943.1574	503882.9	1527.8	71940.4
2	'HEOS::Water'	2.0000	294000.0	348.1	974.9291	314232.1	1015.6	27325.5
3	'HEOS::Water'	2.0000	300000.0	348.2	974.9312	314240.9	1015.6	27332.2
4	'HEOS::Isobutane'	0.8656	267240.7	288.2	562.9619	234945.5	1123.8	30167.3
5	'HEOS::Isobutane'	0.8656	1696290.9	289.3	564.2429	238566.0	1127.6	32723.7
6	'HEOS::Isobutane'	0.8656	1696290.9	289.3	564.2429	238566.0	1127.6	32723.7
7	'HEOS::Isobutane'	0.8656	1662365.1	366.9	44.3350	676756.1	2393.9	112359.2
8	'HEOS::Isobutane'	0.8656	272694.6	317.3	6.3921	625618.1	2464.3	41283.0
9	'HEOS::Isobutane'	0.8656	272694.6	317.3	6.3921	625618.1	2464.3	41283.0
10	'HEOS::Water'	44.4122	101325.0	283.2	999.7025	42118.9	151.1	0.0
11	'HEOS::Water'	44.4122	103392.9	283.2	999.7034	42121.9	151.1	2.1
12	'HEOS::Water'	44.4122	101325.0	285.0	999.5211	49736.2	177.9	24.3
Design 2 with recuperator								
1	'HEOS::Water'	2.0000	300000.0	393.2	943.1574	503882.9	1527.8	71940.4
2	'HEOS::Water'	2.0000	294000.0	348.1	974.9291	314232.1	1015.6	27325.5
3	'HEOS::Water'	2.0000	300000.0	348.2	974.9312	314240.9	1015.6	27332.2
4	'HEOS::Isobutane'	0.9590	267240.7	288.2	562.9619	234945.5	1123.8	30167.3
5	'HEOS::Isobutane'	0.9590	1381487.6	289.0	563.9634	237769.4	1126.8	32160.7
6	'HEOS::Isobutane'	0.9590	1353857.9	323.0	519.6984	321725.5	1401.3	38371.4
7	'HEOS::Isobutane'	0.9590	1326780.7	378.4	30.0529	717253.4	2527.5	115028.1
8	'HEOS::Isobutane'	0.9590	278259.8	340.1	6.0107	668017.0	2590.6	47931.7
9	'HEOS::Isobutane'	0.9590	272694.6	294.0	7.0384	584060.9	2328.3	38227.6
10	'HEOS::Water'	47.2096	101325.0	283.2	999.7025	42118.9	151.1	0.0
11	'HEOS::Water'	47.2096	103392.9	283.2	999.7034	42121.9	151.1	2.1
12	'HEOS::Water'	47.2096	101325.0	284.8	999.5349	49213.5	176.1	21.1

4.3 Case Study 3: Biomass

Four optimization runs have been performed for Case Study 3:

- Design 1
- Design 1 with recuperator
- Design 2
- Design 2 with recuperator

and Figure 10 shows the temperature-enthalpy diagrams of the optimal operating conditions. The detailed stream conditions are included at the end of this chapter (Table 16). The values of the variables and constraints from the optimal solutions are also shown in Appendix A.3.

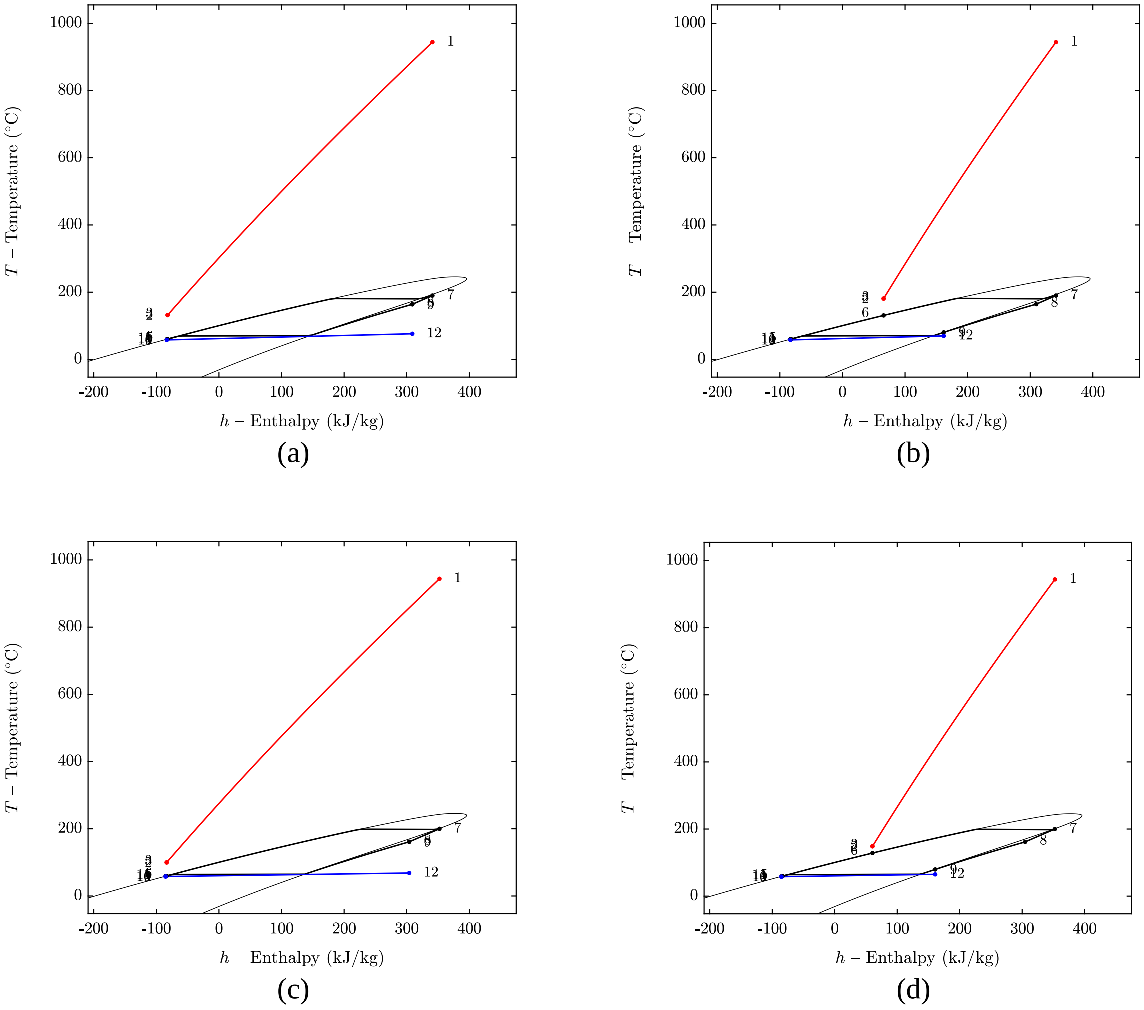

Figure 10. Temperature-enthalpy diagram of optimized Case study 3. (a) Design 1, (b) Design 1 with recuperator, (c) Design 2, (d) Design 2 with recuperator.

Table 17. System performance of Case Study 3.

Parameter	Unit	design 1	design 1 rec	design 2	design 2 rec
W_exp	kW	6.98	9.94	10.55	14.70
W_pump_h	kW	0.03	0.04	0.03	0.03
W_pump_f	kW	0.26	0.39	0.36	0.54
W_pump_c	kW	0.02	0.02	0.03	0.04
W_net	kW	6.67	9.49	10.13	14.08
eta_plant_energy	%	5.84	8.31	8.88	12.34
eta_cycle_energy	%	7.27	10.95	10.67	15.64
eta_plant_exergy	%	11.14	15.85	16.93	23.53
eta_cycle_exergy	%	11.67	17.12	17.46	24.88

Table 17 shows the comparison in terms of efficiency for each of Design 1 and 2, with and without a recuperator. The optimal solution of Design 2 with a recuperator gives the highest energy and exergy efficiency. It is worth noting that considering the quality of heat collected from the heat source, the exergy efficiencies tend to have a higher value than energy based efficiencies. As seen in Table 17, not restricting the design to rig constraints provides higher efficiency in the optimized thermodynamic cycle design. In addition, including a recuperator in the cycle configuration increases the plant and cycle efficiency. Design 1 with recuperator even gives almost the same net power production as Design 2 where the ORC system is operated under practical limits.

Table 18. Expander parameters for optimized Case Study 3.

Parameter	Unit	design 1	design 1 rec	design 2	design 2 rec
Isentropic efficiency	-	0.55	0.55	0.70	0.70
Power output	kW	6.98	9.94	10.55	14.70
Pressure ratio	-	16.31	15.50	27.73	26.34
Diameter	cm	8.82	10.41	9.40	10.95
Rpm	rpm	52377.08	43953.11	53425.82	45511.32
T_{exp_in}	°C	190 (max 190)	190 (max 190)	200 (max 200)	200 (max 190)
P_{exp_in}	bara	6.4 (max 8)	6.4 (max 8)	8.9 (max 10)	8.9 (max 10)
P_{exp_out}	bara	0.4 (min 0.2)	0.4 (min 0.2)	0.3 (min 0.12)	0.3 (min 0.12)

The results from the thermodynamic optimization and resulting expander design parameters are presented in Table 18. The power output of the expander in Case Study 3 is ranged from around 7 to 15 kW. The expander has a high pressure ratio for both Design 1 and 2 due to the low expander outlet pressure level. Preliminary estimation of expander design with the thermodynamic optima of the ORC system gives the diameter from ca. 9 to 11 cm and the RPM ca. from 45000 to 54000, which are acceptable values for small-scale expanders. For all cases, the expander inlet temperature reaches the upper limit, indicating that increasing turbine inlet temperature is the key factor for further improvement of the ORC system. Assuming a simple configuration, **the expander design parameters for further consideration in WP2 should be the ones for Design 1**, representing boundary conditions and design parameters for a simple ORC cycle with MM as working fluid, considering the expander rig constraints at the CTU test rig.

The resulting heat duty, LMTD, and size (UA) of the evaporator, condenser, and recuperator are presented in Figure 11. For all cases, the heat duty of the evaporator and the condenser are at a similar level for this case study. However, due to the high temperature heat source (biomass combustion flue gas), the LMTD in the evaporator is significantly larger than other heat exchangers, resulting in a smaller UA value. It is worth noting that the UA value of the recuperator is also marginal compared to the condenser. Thus, in this case study, the use of a recuperator will deliver a larger power output with a slightly increased capital cost, improving the economic feasibility of the additional heat exchanger.

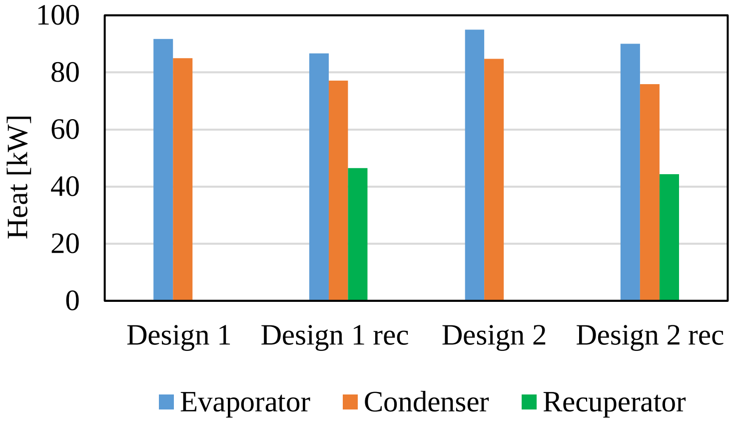

(a)

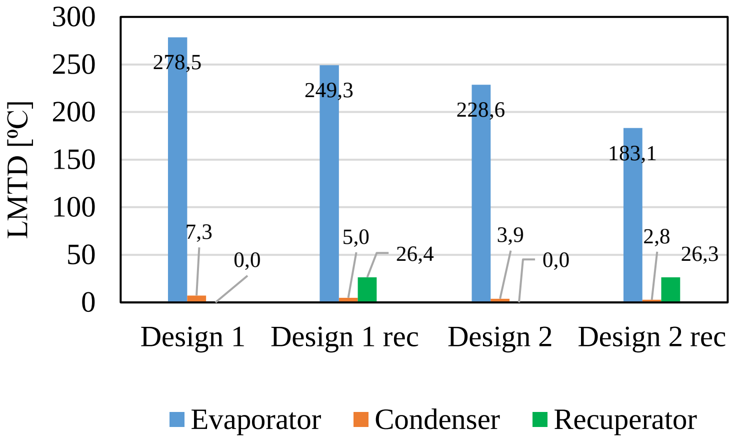

(b)

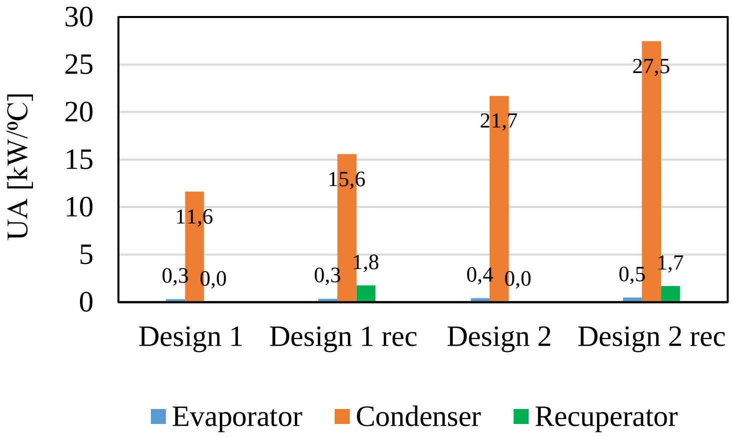

(c)

Figure 11. Heat exchanger parameters for optimized Case Study 3. (a) Heat duty, (b) LMTD, (c) UA.

Table 19 Stream conditions for optimized Case study 3.

Stream	fluid* [-]	m [kg/s]	p [Pa]	T [K]	d [kg/m3]	h [J/kg]	s [J/kg/K]	e [J/kg]
Design 1								
1	REFPROP::flue gas'	0.0963	101325.0	1217.2	0.2917	1510062.5	8029.5	621548.8
2	REFPROP::flue gas'	0.0963	101070.0	404.8	0.8750	557554.8	6761.0	28203.7
3	REFPROP::flue gas'	0.0963	101325.0	405.2	0.8765	557897.4	6761.1	28510.3
4	'HEOS::MM'	0.2167	37394.2	333.2	721.7342	-83251.7	-235.4	7621.7
5	'HEOS::MM'	0.2167	675876.2	333.5	722.6870	-82073.1	-234.6	8550.2
6	'HEOS::MM'	0.2167	675876.2	333.5	722.6870	-82073.1	-234.6	8550.2
7	'HEOS::MM'	0.2167	642082.4	463.2	34.3865	341101.5	788.6	142022.2
8	'HEOS::MM'	0.2167	39362.3	437.1	1.7823	308919.8	849.7	92537.9
9	'HEOS::MM'	0.2167	39362.3	437.1	1.7823	308919.8	849.7	92537.9
10	'HEOS::Water'	1.1127	210000.0	331.2	984.2603	242971.4	806.0	15412.0
11	'HEOS::Water'	1.1127	221052.6	331.2	984.2645	242986.4	806.0	15423.7
12	'HEOS::Water'	1.1127	210000.0	349.4	974.1446	319380.0	1030.6	28224.1
Design 1 with recuperator								
1	REFPROP::flue gas'	0.0963	101325.0	1217.2	0.2917	1510062.5	8029.5	621548.8
2	REFPROP::flue gas'	0.0963	101070.0	454.0	0.7802	610067.1	6883.4	46053.8
3	REFPROP::flue gas'	0.0963	101325.0	454.3	0.7815	610451.3	6883.5	46402.1
4	'HEOS::MM'	0.3147	37394.2	333.2	721.7342	-83251.7	-235.4	7621.7
5	'HEOS::MM'	0.3147	711448.6	333.5	722.7396	-82007.5	-234.5	8601.9
6	'HEOS::MM'	0.3147	675876.2	404.0	638.3675	65707.1	166.8	42690.4
7	'HEOS::MM'	0.3147	642082.4	463.2	34.3865	341101.5	788.6	142022.2
8	'HEOS::MM'	0.3147	41434.0	437.5	1.8759	309522.4	848.5	93483.9
9	'HEOS::MM'	0.3147	39362.3	353.5	2.2398	161807.8	477.0	50954.0
10	'HEOS::Water'	1.5491	210000.0	331.2	984.2603	242971.4	806.0	15412.0
11	'HEOS::Water'	1.5491	221052.6	331.2	984.2645	242986.4	806.0	15423.7
12	'HEOS::Water'	1.5491	210000.0	343.0	977.8727	292770.1	953.7	23377.3
Design 2								
1	REFPROP::flue gas'	0.0963	101325.0	1217.2	0.2917	1510062.5	8029.5	621548.8
2	REFPROP::flue gas'	0.0963	101070.0	372.9	0.9502	523666.0	6673.8	19005.3
3	REFPROP::flue gas'	0.0963	101325.0	373.2	0.9519	523981.5	6673.9	19284.9
4	'HEOS::MM'	0.2179	30466.9	332.2	722.8293	-85250.0	-241.4	7316.2
5	'HEOS::MM'	0.2179	936029.9	332.7	724.1627	-83581.4	-240.2	8629.7
6	'HEOS::MM'	0.2179	936029.9	332.7	724.1627	-83581.4	-240.2	8629.7
7	'HEOS::MM'	0.2179	889228.4	473.2	52.0794	352365.5	800.2	150006.1
8	'HEOS::MM'	0.2179	32070.4	434.4	1.4581	303925.4	848.6	87854.8
9	'HEOS::MM'	0.2179	32070.4	434.4	1.4581	303925.4	848.6	87854.8
10	'HEOS::Water'	1.9417	210000.0	331.2	984.2603	242971.4	806.0	15412.0
11	'HEOS::Water'	1.9417	221052.6	331.2	984.2645	242986.4	806.0	15423.7
12	'HEOS::Water'	1.9417	210000.0	341.6	978.6992	286656.8	935.9	22320.7
Design 2 with recuperator								
1	REFPROP::flue gas'	0.0963	101325.0	1217.2	0.2917	1510062.5	8029.5	621548.8
2	REFPROP::flue gas'	0.0963	101070.0	421.5	0.8403	575323.5	6804.0	33793.8
3	REFPROP::flue gas'	0.0963	101325.0	421.8	0.8418	575680.3	6804.1	34114.5
4	'HEOS::MM'	0.3083	30466.9	332.2	722.8293	-85250.0	-241.4	7316.2
5	'HEOS::MM'	0.3083	985294.6	332.7	724.2343	-83490.7	-240.1	8701.1
6	'HEOS::MM'	0.3083	936029.9	401.5	642.7245	60393.7	152.6	41398.3
7	'HEOS::MM'	0.3083	889228.4	473.2	52.0794	352365.5	800.2	150006.1
8	'HEOS::MM'	0.3083	33758.3	434.8	1.5342	304694.2	847.8	88857.8
9	'HEOS::MM'	0.3083	32070.4	352.7	1.8192	160809.7	484.4	47864.5
10	'HEOS::Water'	2.6080	210000.0	331.2	984.2603	242971.4	806.0	15412.0
11	'HEOS::Water'	2.6080	221052.6	331.2	984.2645	242986.4	806.0	15423.7
12	'HEOS::Water'	2.6080	210000.0	338.1	980.6242	272071.8	893.0	19887.7

4.4 Case summary

The optimal solutions of the three case studies (biogas, geothermal, and biomass) are compared in this Chapter. Figure 12 presents that the biogas (Case Study 1) and the biomass (Case Study 3) cases have a larger benefit of using a recuperator than the geothermal case. Under the practical constraints (Design 2), the biomass case shows the highest increase rate in the net power production (over 50 %). Therefore, adding a recuperator and pushing operating conditions to technical limits could be effective options to improve the performance of small-scale ORC systems for the biomass and the biogas cases.

Regarding the system efficiency, all case studies have very low cycle energy efficiency below 20 % as seen in Figure 13. In addition, the geothermal case has the lowest cycle energy efficiency. However, if the quality of the heat source is considered (i.e., exergy), the ORC of the geothermal case shows the best thermodynamic performance with the cycle exergy efficiency of ca. 50 %. As indicated in Chapter 4.1 and 4.3, the biogas and the biomass cases have extremely high heat source temperatures and relatively low working fluid temperatures in the evaporator, and these result in significantly large LMTD and entropy generation in the heat exchanger, reducing the thermodynamic performance of the ORC.

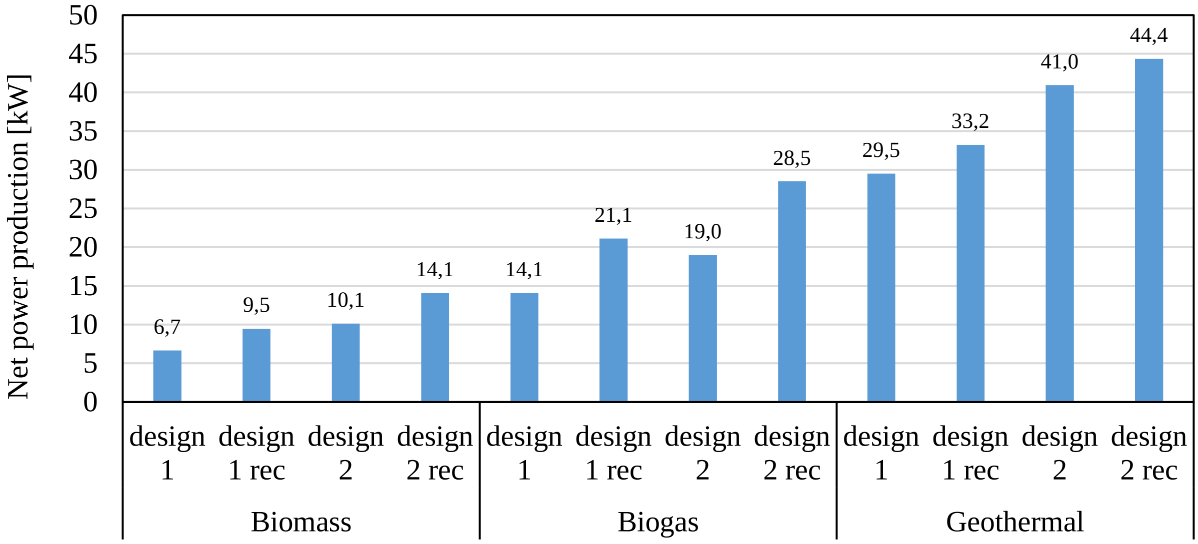

Figure 12. Net power production of the optimized case studies.

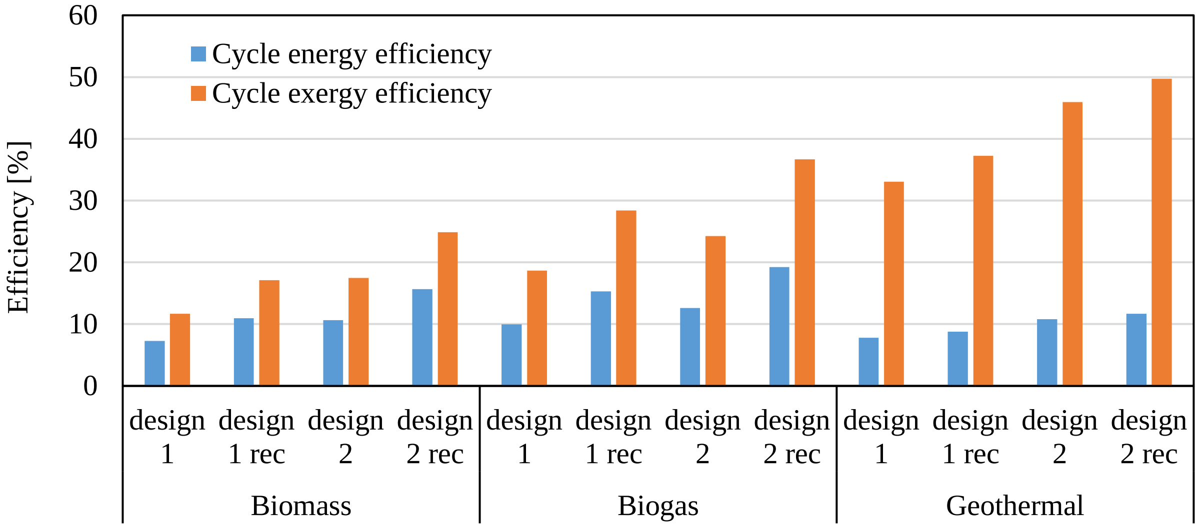

Figure 13. Cycle efficiency of the optimized case studies.

Figure 14 presents that the biogas and biomass cases also have a significantly higher pressure ratio due to the low expander outlet pressure level (see Chapter 4.1 and 4.3) compared to the geothermal case. As seen in Figure 15, the expander diameter and rotational speed of the case studies are ranged from 10 to 20 cm and from 30000 to 60000 rpm, which are typical values for small-scale expanders. It is worth noting that the biogas case has a larger diameter, but a lower rpm compared to other cases. However, the expander diameter and rotational speed are based on preliminary analysis with assumptions. Thus, the two expander parameters will be tuned with detailed expander models in WP2.

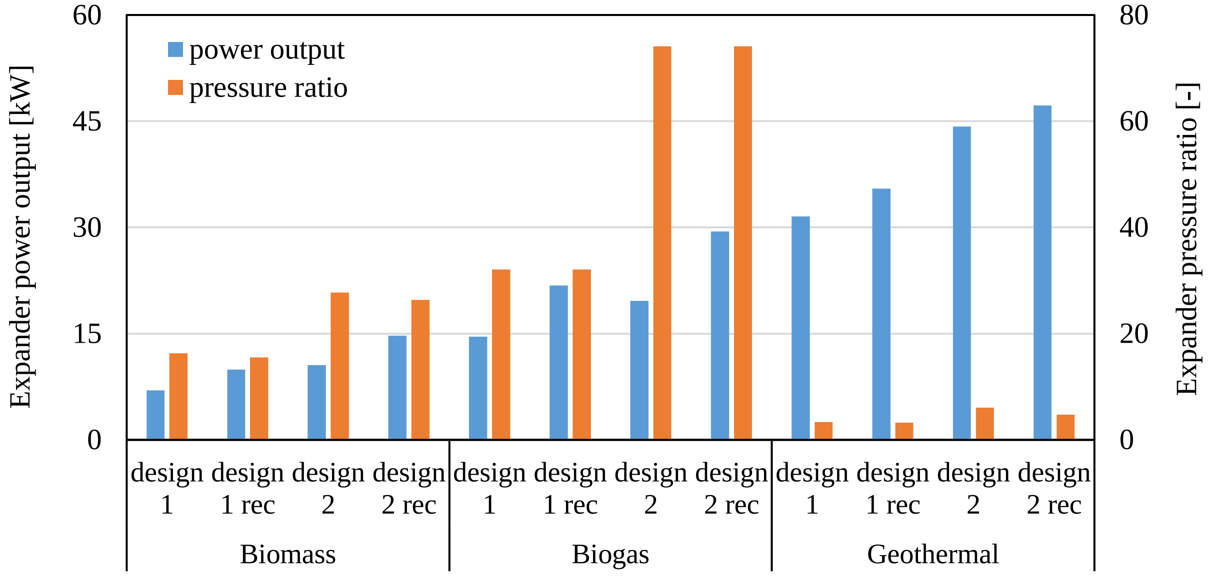

Figure 14. Expander power output and pressure ratio in the optimized case studies.

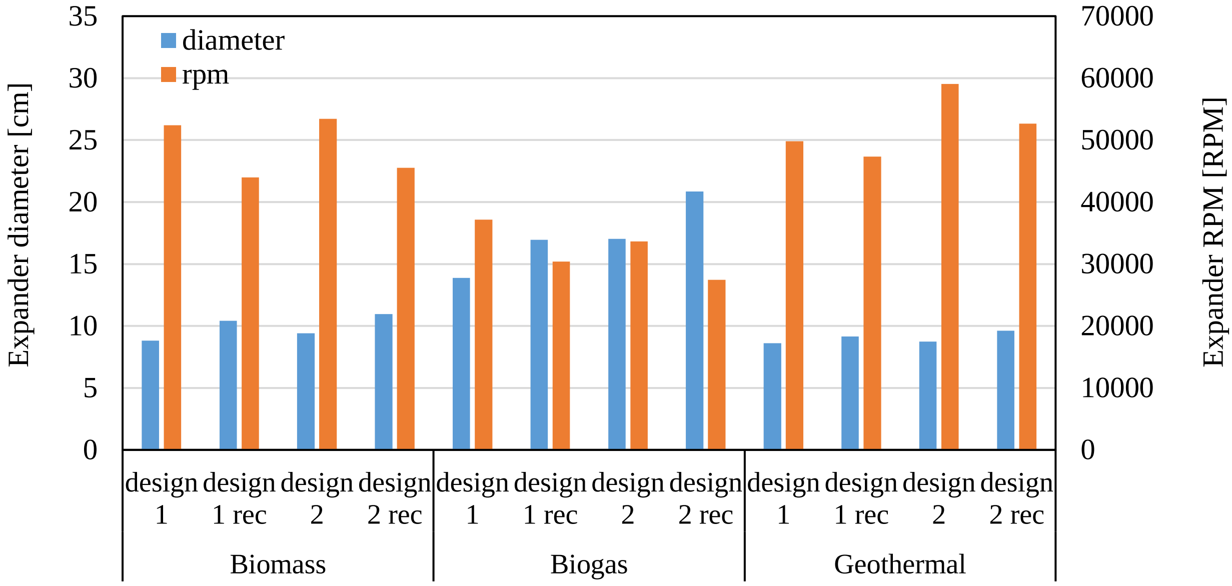

Figure 15. Preliminary diameter and rotating speed of the expander in the optimized case studies.

5 Conclusions

First law efficiency (cycle energy efficiency) is ca. 10 % for all case studies under simple cycle configurations, and this is well explained by Carnot efficiency limitations due to the low temperature value in heat source, together with the rig constraints. Overall, this leads to very low cycle efficiencies in small scale ORC applications regardless of the application. However, if we consider the quality of the heat sources, the exergy efficiency is varied from 10 to 40 %, indicating that the use of a recuperator and the practical constraints will be the key factors to improve the thermodynamic performance of the small-scale ORC systems.

The optimization results and preliminary expander design analysis indicate the dimension and rotating speed of the turbomachinery is within the typical design range of such small gas expanders. Thus, the results from this WP1 give input parameters to WP2 that could be used as first estimate boundary and operating conditions for detail expander design in other work packages. As the expander design activities in WP2 proceed, further communication between WP1 and WP2 are envisaged to refine and mutually strengthen the work.

Appendix A

A.1 Case study 1

Table 20. Variable values from the optimal solutions of Case study 1.

Variable name	Lower bound	Variable value	Upper bound
Design 1			
Heat source exit temperature	0	0.0000	1
Heat sink exit temperature	0	1.0000	1
Pump inlet pressure	0	0.0180	1
Pump inlet enthalpy	0	0.0264	1
Expander inlet pressure	0	0.6417	1
Expander inlet enthalpy	0	0.2765	1
Recuperator effectiveness	0	0.0000	0
Design 1 Rec.			
Heat source exit temperature	0	0.0248	1
Heat sink exit temperature	0	1.0000	1
Pump inlet pressure	0	0.0171	1
Pump inlet enthalpy	0	0.0441	1
Expander inlet pressure	0	0.6417	1
Expander inlet enthalpy	0	0.4866	1
Recuperator effectiveness	0	0.6708	0
Design 2			
Heat source exit temperature	0	0.0000	1
Heat sink exit temperature	0	1.0000	1
Pump inlet pressure	0	0.0104	1
Pump inlet enthalpy	0	0.0186	1
Expander inlet pressure	0	0.8891	1
Expander inlet enthalpy	0	0.2826	1
Recuperator effectiveness	0	0.0000	0
Design 2 Rec.			
Heat source exit temperature	0	0.0156	1
Heat sink exit temperature	0	1.0000	1
Pump inlet pressure	0	0.0008	1
Pump inlet enthalpy	0	0.0175	1
Expander inlet pressure	0	0.8881	1
Expander inlet enthalpy	0	0.2826	1
Recuperator effectiveness	0	0.6752	1

Table 21. Constraint values from the optimal solutions of Case study 1.

Constraint	Unit	Lower bound	Constraint value	Upper bound
Design 1				
Evaporator pinch point	°C	50.00	116.99	-
Condenser pinch point	°C	2.00	25.32	-
Recuperator pinch point	°C	20.00	112.86	-
Expander vapor quality	-	1.00	1.10	-
Pump inlet subcooling	°C	9.60	9.60	-
Expander inlet superheating	°C	10.00	10.00	-
Expander power	kW	-	14.58	50.00
Expander inlet p	bara	-	6.42	8.00
Expander inlet T	°C	-	190.00	190.00
Expander outlet p	bara	0.20	0.20	-
Design 1 Rec.				
Evaporator pinch point	°C	50.00	50.00	-
Condenser pinch point	°C	2.00	24.07	-
Recuperator pinch point	°C	20.00	20.00	-
Expander vapor quality	-	1.00	1.10	-
Pump inlet subcooling	°C	9.60	9.60	-
Expander inlet superheating	°C	10.00	10.00	-
Expander power	kW	-	21.81	50.00
Expander inlet p	bara	-	6.42	8.00
Expander inlet T	°C	-	190.00	190.00
Expander outlet p	bara	0.20	0.20	-
Design 2				
Evaporator pinch point	°C	20.00	94.20	-
Condenser pinch point	°C	1.00	17.99	-
Recuperator pinch point	°C	20.00	117.52	-
Expander vapor quality	-	1.00	1.10	-
Pump inlet subcooling	°C	5.00	5.00	-
Expander inlet superheating	°C	2.00	2.00	-
Expander power	kW	-	19.64	50.00
Expander inlet p	bara	-	8.89	10.00
Expander inlet T	°C	-	200.00	200.00
Expander outlet p	bara	0.12	0.12	-
Design 2 Rec.				
Evaporator pinch point	°C	20.00	20.00	-
Condenser pinch point	°C	1.00	13.90	-
Recuperator pinch point	°C	20.00	20.00	-
Expander vapor quality	-	1.00	1.10	-
Pump inlet subcooling	°C	5.00	5.00	-
Expander inlet superheating	°C	2.00	2.00	-
Expander power	kW	-	29.45	50.00
Expander inlet p	bara	-	8.89	10.00
Expander inlet T	°C	-	200.00	200.00
Expander outlet p	bara	0.12	0.12	-

A.2 Case study 2

Table 22. Variable values from the optimal solutions of Case study 2.

Variable name	Lower bound	Variable value	Upper bound
Design 1			
Heat source exit temperature	0	0.0000	1
Heat sink exit temperature	0	0.6529	1
Pump inlet pressure	0	0.0322	1
Pump inlet enthalpy	0	0.0426	1
Expander inlet pressure	0	0.1102	1
Expander inlet enthalpy	0	0.8089	1
Recuperator effectiveness	0	0.0000	0
Design 1 Rec.			
Heat source exit temperature	0	0.0000	1
Heat sink exit temperature	0	0.5907	1
Pump inlet pressure	0	0.0322	1
Pump inlet enthalpy	0	0.0426	1
Expander inlet pressure	0	0.1076	1
Expander inlet enthalpy	0	0.8541	1
Recuperator effectiveness	0	0.5671	0
Design 2			
Heat source exit temperature	0	0.0000	1
Heat sink exit temperature	0	0.1816	1
Pump inlet pressure	0	0.0245	1
Pump inlet enthalpy	0	0.0211	1
Expander inlet pressure	0	0.1527	1
Expander inlet enthalpy	0	0.8133	1
Recuperator effectiveness	0	0.0000	0
Design 2 Rec.			
Heat source exit temperature	0	0.0000	1
Heat sink exit temperature	0	0.1692	1
Pump inlet pressure	0	0.0245	1
Pump inlet enthalpy	0	0.0211	1
Expander inlet pressure	0	0.1219	1
Expander inlet enthalpy	0	0.8859	1
Recuperator effectiveness	0	0.6465	1

Table 23. Constraint values from the optimal solutions of Case study 2.

Constraint	Unit	Lower bound	Constraint value	Upper bound
Design 1				
Evaporator pinch point	°C	10.00	15.46	-
Condenser pinch point	°C	10.00	10.00	-
Recuperator pinch point	°C	10.00	32.24	-
Expander vapor quality	-	1.00	1.10	-
Pump inlet subcooling	°C	5.00	5.00	-
Expander inlet superheating	°C	5.00	10.08	-
Expander power	kW	-	31.55	50.00
Expander inlet p	bara	-	12.00	12.00
Expander inlet T	°C	-	84.66	150.00
Expander outlet p	bara	1.50	3.58	-
Design 1 Rec.				
Evaporator pinch point	°C	10.00	10.00	-
Condenser pinch point	°C	10.00	10.00	-
Recuperator pinch point	°C	10.00	10.00	-
Expander vapor quality	-	1.00	1.10	-
Pump inlet subcooling	°C	5.00	5.00	-
Expander inlet superheating	°C	5.00	21.89	-
Expander power	kW	-	35.50	50.00
Expander inlet p	bara	-	11.72	12.00
Expander inlet T	°C	-	95.36	150.00
Expander outlet p	bara	1.50	3.65	-
Design 2				
Evaporator pinch point	°C	5.00	5.00	-
Condenser pinch point	°C	5.00	5.00	-
Recuperator pinch point	°C	5.00	28.07	-
Expander vapor quality	-	1.00	1.10	-
Pump inlet subcooling	°C	1.00	1.00	-
Expander inlet superheating	°C	2.00	3.16	-
Expander power	kW	-	44.27	50.00
Expander inlet p	bara	-	16.62	50.00
Expander inlet T	°C	-	93.80	150.00
Expander outlet p	bara	0.50	2.73	-
Design 2 Rec.				
Evaporator pinch point	°C	5.00	5.00	-
Condenser pinch point	°C	5.00	5.00	-
Recuperator pinch point	°C	5.00	5.00	-
Expander vapor quality	-	1.00	1.10	-
Pump inlet subcooling	°C	1.00	1.00	-
Expander inlet superheating	°C	2.00	25.89	-
Expander power	kW	-	47.22	50.00
Expander inlet p	bara	-	13.27	50.00
Expander inlet T	°C	-	105.27	150.00
Expander outlet p	bara	0.50	2.78	-

A.3 Case study 3

Table 24. Enthalpy difference between actual flue gas and estimated flue gas with correction factor.

Temperature range [°C]		dh [kJ/kg]		Error [%]
From	To	Actual flue gas	Estimated flue gas× 1.234536*	
100	200	131.60	131.81	0.16
200	300	134.90	134.96	0.04
300	400	138.40	138.49	0.07
400	500	142.10	142.13	0.02
500	600	145.70	145.70	0.00
600	700	149.00	148.89	0.08
700	800	152.10	152.09	0.00
800	900	155.00	154.56	0.28
900	1000	157.90	157.03	0.55

* This factor is used to estimate mass flow rate of the flue gas (actual flue gas mass flow rate×1.234536)

Table 25. Variable values from the optimal solutions of Case study 3.

Variable name	Lower bound	Variable value	Upper bound
Design 1			
Heat source exit temperature	0	0.0000	1
Heat sink exit temperature	0	0.6757	1
Pump inlet pressure	0	0.0374	1
Pump inlet enthalpy	0	0.0521	1
Expander inlet pressure	0	0.6421	1
Expander inlet enthalpy	0	0.2816	1
Recuperator effectiveness	0	0.0000	0
Design 1 Rec.			
Heat source exit temperature	0	0.0605	1
Heat sink exit temperature	0	0.4405	1
Pump inlet pressure	0	0.0374	1
Pump inlet enthalpy	0	0.0912	1
Expander inlet pressure	0	0.6421	1
Expander inlet enthalpy	0	0.4930	1
Recuperator effectiveness	0	0.6597	0
Design 2			
Heat source exit temperature	0	0.0000	1
Heat sink exit temperature	0	0.3865	1
Pump inlet pressure	0	0.0305	1
Pump inlet enthalpy	0	0.0510	1
Expander inlet pressure	0	0.8892	1
Expander inlet enthalpy	0	0.2877	1
Recuperator effectiveness	0	0.0000	0
Design 2 Rec.			
Heat source exit temperature	0	0.0577	1
Heat sink exit temperature	0	0.2575	1
Pump inlet pressure	0	0.0305	1
Pump inlet enthalpy	0	0.0510	1
Expander inlet pressure	0	0.8892	1
Expander inlet enthalpy	0	0.2877	1
Recuperator effectiveness	0	0.6569	1

Table 26. Constraint values from the optimal solutions of Case study 3.

Constraint	Unit	Lower bound	Constraint value	Upper bound
Design 1				
Evaporator pinch point	°C	50.00	71.30	-
Condenser pinch point	°C	2.00	2.00	-
Recuperator pinch point	°C	20.00	103.61	-
Expander vapor quality	-	1.00	1.10	-
Pump inlet subcooling	°C	9.60	9.60	-
Expander inlet superheating	°C	10.00	10.00	-
Expander power	kW	-	6.98	15.50
Expander inlet p	bara	-	6.42	8.00
Expander inlet T	°C	-	190.00	190.00
Expander outlet p	bara	0.20	0.39	-
Design 1 Rec.				
Evaporator pinch point	°C	50.00	50.00	-
Condenser pinch point	°C	2.00	2.00	-
Recuperator pinch point	°C	20.00	20.00	-
Expander vapor quality	-	1.00	1.10	-
Pump inlet subcooling	°C	9.60	9.60	-
Expander inlet superheating	°C	10.00	10.00	-
Expander power	kW	-	9.94	15.50
Expander inlet p	bara	-	6.42	8.00
Expander inlet T	°C	-	190.00	190.00
Expander outlet p	bara	0.20	0.41	-
Design 2				
Evaporator pinch point	°C	20.00	40.17	-
Condenser pinch point	°C	1.00	1.00	-
Recuperator pinch point	°C	20.00	101.67	-
Expander vapor quality	-	1.00	1.10	-
Pump inlet subcooling	°C	5.00	5.00	-
Expander inlet superheating	°C	2.00	2.00	-
Expander power	kW	-	10.55	50.00
Expander inlet p	bara	-	8.89	10.00
Expander inlet T	°C	-	200.00	200.00
Expander outlet p	bara	0.12	0.32	-
Design 2 Rec.				
Evaporator pinch point	°C	20.00	20.00	-
Condenser pinch point	°C	1.00	1.00	-
Recuperator pinch point	°C	20.00	20.00	-
Expander vapor quality	-	1.00	1.10	-
Pump inlet subcooling	°C	5.00	5.00	-
Expander inlet superheating	°C	2.00	2.00	-
Expander power	kW	-	14.70	50.00
Expander inlet p	bara	-	8.89	10.00
Expander inlet T	°C	-	200.00	200.00
Expander outlet p	bara	0.12	0.34	-